



Diffusion-controlled coalescence, fragmentation, and collapse of d -dimensional A -particle islands in the B -particle sea

Boris M. Shipilevsky 

Institute of Solid State Physics, Chernogolovka, Moscow district, 142432, Russia

 (Received 3 September 2019; revised manuscript received 31 October 2019; published 16 December 2019)

We present a systematic analysis of diffusion-controlled interaction and collapse of two identical spatially separated d -dimensional A -particle islands in the B -particle sea at propagation of the sharp reaction front $A + B \rightarrow 0$ at equal species diffusivities. We show that at a sufficiently large initial distance between the centers of islands 2ℓ compared to their characteristic initial size and a relatively large initial ratio of island to sea concentrations, the evolution dynamics of the island-sea-island system is determined unambiguously by the dimensionless parameter $\Lambda = \mathcal{N}_0/\mathcal{N}_\Omega$, where \mathcal{N}_0 is the initial particle number in the island and \mathcal{N}_Ω is the initial number of sea particles in the volume $\Omega = (2\ell)^d$. It is established that (a) there is a d -dependent critical value Λ_* above which island coalescence occurs; (b) regardless of d the centers of each of the islands move toward each other along a *universal* trajectory merging in a united center at the d -dependent critical value $\Lambda_s \geq \Lambda_*$; (c) in one-dimensional systems $\Lambda_* = \Lambda_s$, therefore, at $\Lambda < \Lambda_*$ each of the islands dies individually, whereas at $\Lambda > \Lambda_*$ coalescence is completed by collapse of a single-centered island in the system center; (d) in two- and three-dimensional systems in the range $\Lambda_* < \Lambda < \Lambda_s$ coalescence is accompanied by subsequent fragmentation of a two-centered island and is completed by individual collapse of each of the islands. We discuss a detailed picture of coalescence, fragmentation, and collapse of islands focusing on evolution of their shape and on behavior of the relative width of the reaction front at the final collapse stage and in the vicinity of starting coalescence and fragmentation points. We demonstrate that in a wide range of parameters, the front remains sharp up to a narrow vicinity of the coalescence, fragmentation, and collapse points.

DOI: [10.1103/PhysRevE.100.062121](https://doi.org/10.1103/PhysRevE.100.062121)

I. INTRODUCTION

The fundamental reaction-diffusion system $A + B \rightarrow 0$, where unlike species A and B diffuse and irreversibly annihilate in the bulk of a d -dimensional medium, has attracted great interest in recent decades owing to the remarkable property of *effective dynamical repulsion* of unlike species [1–6]. In unbounded systems with initially statistically homogeneous particle distribution, this property brings about spontaneous growth of A and B particles domains (Ovchinnikov-Zeldovich segregation) and, as a consequence, anomalous reaction deceleration. In systems with initially spatially separated reactants this property results in the formation and self-similar propagation of a localized reaction front which, depending on the interpretation of A and B (chemical reagents, quasiparticles, topological defects, etc.), plays a key role in a broad spectrum of problems in physics, chemistry, biology, and materials science [7–15].

The simplest model of a planar reaction front, introduced by Galfi and Racz (GR) [16] is the quasi-one-dimensional model for two initially separated reactants which are uniformly distributed on the left side ($x < 0$) and on the right side ($x > 0$) of the initial boundary. Taking the reaction rate in the mean-field form $R(x, t) = ka(x, t)b(x, t)$ (k being the reaction constant), GR discovered that in the long time limit $kt \gg 1$ the reaction profile $R(x, t)$ acquires the universal scaling form

$$R = R_f \mathcal{R}\left(\frac{x - x_f}{w}\right),$$

where x_f , R_f , and w are, respectively, position, height, and width of the reaction front and the front width anomalously slowly grows with time by the law

$$w \propto (t/k^2)^{1/6},$$

so that on the diffusion length scale $\propto t^{1/2}$ the relative width of the front asymptotically contracts unlimitedly $\propto (kt)^{-1/3} \rightarrow 0$ as $kt \rightarrow \infty$. Subsequently, it was shown [17–21] that the mean-field approximation is valid at $d > d_c = 2$, whereas in one-dimensional systems fluctuations play the dominant role. Nevertheless, the self-similar front motion takes place at all dimensions so that at any d on the diffusion length scale the relative front width contracts asymptotically. Based on this fact, a general concept of the front dynamics for nonzero diffusivities, the quasistatic approximation (QSA), was developed [17,18,21,22]. The key property of the QSA is that the front width $w(J)$ depends on t only through the time-dependent boundary current $J_A = |J_B| = J$, the calculation of which is reduced to solving the external diffusion problem with the moving *absorbing boundary* (Stefan problem)

$$R = J\delta(x - x_f).$$

On the basis of the QSA a general description of spatiotemporal behavior of the system $A + B \rightarrow 0$ has been obtained for arbitrary nonzero diffusivities [23] which was then generalized to the cases of anomalous diffusion [24,25], diffusion in disordered systems [26,27], diffusion in systems with inhomogeneous initial conditions [28], and to several more complex reactions. Following this approach, in most

subsequent works the use of the QSA was traditionally restricted by the quasi-one-dimensional sea-sea problem with A and B domains having an unlimited extension, i.e., with an unlimited number of A and B particles, where asymptotically the stage of monotonous quasistatic front propagation is always reached.

Recently, a new line in the study of the $A + B \rightarrow 0$ front dynamics has attracted significant attention under the assumption that the particle number of one or both species is *finite* (island-sea and island-island systems) and, therefore, in the final state one or both islands *disappear* completely [29–37]. It has been demonstrated that in the sharp-front regime these systems exhibit rich scaling behavior, and though in these systems the QSA is always asymptotically violated, at large initial particle numbers and a high reaction constant the vast majority of particles die in the *sharp-front* regime over a wide parameter range. Here, we will focus mainly on the island-sea system, introduced originally in Ref. [29] for quasi-one-dimensional geometry (flat front) and generalized for d dimensions (ring-shaped or spherical fronts) in the recent Ref. [37]. This system is a basic model for a wide range of phenomena and is realized in numerous applications from Liesegang patterns formation [38–41] to electron-hole luminescence in quantum wells [7–9] depending on the conditions of initial island formation.

Two related island-sea problems were considered at equal species diffusivities in Ref. [37]: (i) the evolution and collapse of an initially uniform d -dimensional spherical A -particle island “submerged” into the uniform d -dimensional B -particle sea and (ii) the formation of a d -dimensional spherical A -particle island from a localized A -particle source acting a finite time in the d -dimensional initially uniform B -particle sea and subsequent evolution and collapse of the island after source switching off in the long-living island regime when the island collapse time t_c exceeds significantly the duration of source action. It has been established that at sufficiently large starting number of A particles \mathcal{N}_0 (where \mathcal{N}_0 is the initial number of A particles in the initially uniform island or the number of injected A particles at the moment of source switching off) and a sufficiently large reaction constant k the death of majority of island particles $\mathcal{N}(t)$, regardless of the initial particle distribution, proceeds in the universal scaling regime

$$\mathcal{N} = \mathcal{N}_0 \mathcal{G}(t/t_c),$$

where $t_c \propto \mathcal{N}_0^{2/d}$ is the lifetime of the island in the sharp-front limit and on the final stage of collapse

$$\mathcal{N}/\mathcal{N}_0 \propto \mathcal{T}^{(d+2)/d} \rightarrow 0$$

as $\mathcal{T} = (t_c - t)/t_c \rightarrow 0$. It has been shown that at a relatively large starting ratio of island to sea concentrations, regardless of the starting particle number and the system dimension, while dying, the island first expands to a certain maximal amplitude and then begins to contract by the universal law

$$\zeta_f = r_f/r_f^M = \sqrt{e\tau |\ln \tau|},$$

where $\tau = t/t_c$ and $r_f^M \propto \mathcal{N}_0^{1/d}$ is the island maximal expansion radius at the front turning point

$$t_M = t_c/e.$$

According to Ref. [37], regardless of the system dimension the evolution of the boundary current density J that determines the quasistatic front width $w(J)$ is described by the universal law

$$\mathcal{J} = J/J_M = \sqrt{\frac{|\ln \tau|}{e\tau}},$$

from which it follows that in the mean-field regime the relative front width $\eta = w/r_f$ changes by the law

$$\eta = \eta_M/(e\tau \ln^2 \tau)^{1/3},$$

where at the front turning point $\eta_M \propto 1/\mathcal{N}_0^{2/3d} k^{1/3}$ and, therefore, on the final stage of collapse

$$\eta \sim \left(\frac{\mathcal{T}_Q}{\mathcal{T}}\right)^{2/3},$$

where $\mathcal{T}_Q \propto 1/\mathcal{N}_0^{1/d} \sqrt{k} \rightarrow 0$ as $\mathcal{N}_0, k \rightarrow \infty$. In Ref. [37], an exhaustive analysis of the reaction front relative width evolution for the fluctuation, the logarithmically modified, and the mean-field regimes was presented, and it was demonstrated that in a wide range of parameters at a large enough number of injected or initially uniformly distributed particles the front remains sharp up to a narrow vicinity of the island collapse point, and therefore the whole picture of the evolution and collapse of the island is completely *self-consistent*.

According to Ref. [37], with an increase of the initial particle number in the island, the amplitude of island expansion at the front turning point increases unlimitedly and, therefore, in the presence of *neighboring islands* in the sea [41,42] the scenario described above for the autonomous evolution of the island is realized only as long as the amplitude of the island expansion remains much less than the distance between the centers of neighboring islands. If in the sea there are one or several neighboring islands and this condition is violated, i.e., the amplitude of the island’s expansion becomes comparable with the distance between the centers of the neighboring islands, it is obvious that the dynamics of island evolution must radically change.

In this article, we pose and systematically investigate the problem of diffusion-controlled *interaction* of two identical d -dimensional A -particle islands separated by a sufficiently large initial distance in the d -dimensional B -particle sea. This model is the simplest basic model of the *island-sea-island* system which allows revealing the key features of the evolution dynamics under the assumption of sharp-front formation at equal species diffusivities. Moreover, because of mirror symmetry, this model simultaneously describes the evolution of the d -dimensional A -particle island in a semi-infinite B -particle sea with a reflecting $(d-1)$ -dimensional “wall.” We discover that if the initial distance between the centers of the islands 2ℓ is large enough compared to their characteristic initial size and the initial ratio of island to sea concentrations is relatively large, the evolution dynamics of the island-sea-island system demonstrates remarkable universality and is determined unambiguously by the dimensionless parameter

$$\Lambda = \mathcal{N}_0/\mathcal{N}_\Omega,$$

where \mathcal{N}_0 is the initial particle number in the island and \mathcal{N}_Ω is the initial number of sea particles in the volume $\Omega = (2\ell)^d$.

We show that at $\Lambda^{2/d} \ll 1$ each of the islands evolves and dies *autonomously* not feeling the presence of a neighboring island and demonstrate that there is a d -dependent critical value Λ_* below which each of the islands dies individually and above which island coalescence occurs. We also reveal that there is the second d -dependent critical value $\Lambda_s \geq \Lambda_*$ above which coalescence is completed by collapse of the formed single-centered island in the system center and we discover the remarkable fact that at $d \geq 2$ in the range $\Lambda_* < \Lambda < \Lambda_s$ coalescence is accompanied by subsequent fragmentation of the two-centered island and is completed by individual collapse of each of the islands. We discuss a detailed picture of coalescence, fragmentation, and collapse of the islands, reveal the remarkable properties of universality and self-similarity of the evolution of islands, give a comprehensive picture of the relative front width evolution, and demonstrate that in a wide range of parameters the reaction front remains sharp up to a narrow vicinity of the coalescence, fragmentation, and collapse points.

II. EVOLUTION OF TWO IDENTICAL SPATIALLY SEPARATED d -DIMENSIONAL A -PARTICLE ISLANDS IN THE d -DIMENSIONAL B -PARTICLE SEA

A. Model

We consider a model in which two identical A -particle islands, which for simplicity have the shape of a d -dimensional hypercube with the side $2h$ and the centers of which are located on the x axis at the points $x = \pm\ell$, are surrounded by a uniform unlimited B -particle sea with the initial concentration b_0 . We shall assume that initially in each of the islands A particles are distributed uniformly with the concentration a_0 . We shall also assume that initially the islands have the same spatial orientation and that the coordinate axes with the origin at the point $x = 0$ on the x axis are normal to hypercube “faces” so that full symmetry takes place:

$$x \leftrightarrow -x, y \leftrightarrow -y, z \leftrightarrow -z.$$

Particles A and B diffuse with the diffusion constants $D_{A,B}$, and when meeting they annihilate with some nonzero probability $A + B \rightarrow 0$. In the continuum version, this process can be described by the reaction-diffusion equations

$$\partial a / \partial t = D_A \nabla^2 a - R, \quad \partial b / \partial t = D_B \nabla^2 b - R, \quad (1)$$

where $a(\mathbf{r}, t)$ and $b(\mathbf{r}, t)$ are the mean local concentrations of A and B and $R(\mathbf{r}, t)$ is the macroscopic reaction rate. We shall assume, as usual, that species diffusivities are equal $D_A = D_B = D$. This important condition, due to local conservation of difference concentration $a - b$, leads to a radical simplification that permits to obtain an analytical solution for arbitrary front trajectory (at different species diffusivities $D_A \neq D_B$ an analytical solution of the Stefan problem is possible only for stationary or a monotonically moving front [34]). Then, by measuring the length, time, and concentration in units of h , h^2/D , and b_0 , respectively, and defining the ratio $a_0/b_0 = c$ and the ratio $L = \ell/h \gg 1$, we come from Eq. (1) to the simple diffusion equation for the difference concentration $s(\mathbf{r}, t) = a(\mathbf{r}, t) - b(\mathbf{r}, t)$,

$$\partial s / \partial t = \nabla^2 s, \quad (2)$$

at the initial conditions

$$s_0(|x| \in (L - 1, L + 1)) = c, \quad (3)$$

and $s_0 = -1$ (sea) outside the islands in the 1D case,

$$s_0(|x| \in (L - 1, L + 1), y \in (-1, +1)) = c, \quad (4)$$

and $s_0 = -1$ (sea) outside the islands in the 2D case,

$$s_0(|x| \in (L - 1, L + 1), y, z \in (-1, +1)) = c, \quad (5)$$

and $s_0 = -1$ (sea) outside the islands in the 3D case, with the boundary conditions

$$s(|\mathbf{r}| \rightarrow \infty, t) = -1 \quad (6)$$

and the symmetry conditions

$$\partial_x s|_{x=0} = \partial_y s|_{y=0} = \partial_z s|_{z=0} = 0.$$

B. Universal long-time asymptotics in the sharp-front limit

Exact solution of the problem, Eqs. (2)–(6), has the form

$$s(x, t) + 1 = \frac{(c + 1)}{2} (\mathcal{L}_+ + \mathcal{L}_-) \quad (7)$$

in the one-dimensional (1D) case,

$$s(\mathbf{r}, t) + 1 = \frac{(c + 1)}{2} (\mathcal{L}_+ + \mathcal{L}_-) Q(y, t) \quad (8)$$

in the two-dimensional (2D) case, and

$$s(\mathbf{r}, t) + 1 = \frac{(c + 1)}{2} (\mathcal{L}_+ + \mathcal{L}_-) Q(y, t) Q(z, t) \quad (9)$$

in the three-dimensional (3D) case, where

$$\mathcal{L}_+(x, t) = \text{erf}\left(\frac{L + 1 + x}{2\sqrt{t}}\right) - \text{erf}\left(\frac{L - 1 + x}{2\sqrt{t}}\right), \quad (10)$$

$$\mathcal{L}_-(x, t) = \text{erf}\left(\frac{L + 1 - x}{2\sqrt{t}}\right) - \text{erf}\left(\frac{L - 1 - x}{2\sqrt{t}}\right), \quad (11)$$

and

$$Q(v, t) = \frac{1}{2} \left[\text{erf}\left(\frac{1 + v}{2\sqrt{t}}\right) + \text{erf}\left(\frac{1 - v}{2\sqrt{t}}\right) \right]. \quad (12)$$

As well as in Refs. [29,37], we shall assume that the ratio of island to sea concentrations is large enough, $c \gg 1$ (concentrated island). Below, it will be shown that in the limit of large $c \gg 1$ the “lifetime” of the islands $t_c \gg 1$, so the majority of the A particles die at times $t \gg 1$, when the diffusive length exceeds appreciably the initial island size. The evolution of the islands in such a large- t regime is of principal interest for us here since, as will be demonstrated below, in the limit of large $t \gg 1$, $L \gg 1$, and $c \gg 1$ *regardless of the initial shape, orientation, and sizes* of the islands the asymptotics of island evolution takes a *universal* form which at a given initial sea density is determined unambiguously only by the initial number of particles in the islands (*the instantaneous source regime*) and the initial distance between their centers.

Assuming that the diffusion length $\sqrt{t} \gg 1$ and expanding the functions $\mathcal{L}_+(x, t)$, $\mathcal{L}_-(x, t)$, and $Q(v, t)$ in powers of $1/\sqrt{t}$ we find

$$\mathcal{L}_+(x, t) = \frac{2e^{-(L+x)^2/4t}}{\sqrt{\pi t}} (1 + q_+), \quad (13)$$

$$\mathcal{L}_-(x, t) = \frac{2e^{-(L-x)^2/4t}}{\sqrt{\pi t}}(1 + q_-), \quad (14)$$

$$Q(v, t) = \frac{e^{-v^2/4t}}{\sqrt{\pi t}} \left(1 - \frac{(1 - v^2/2t)}{12t} + \dots \right), \quad (15)$$

where

$$q_{\pm} = \frac{1}{12t} \left[\frac{(L \pm x)^2}{2t} - 1 \right] + \dots,$$

and the terms of a higher order of smallness in powers of $1/t$, $(L \pm x)^2/t^2$, and v^2/t^2 , respectively, are omitted (following the leading term in q_{\pm} has the form

$$\frac{1}{160t^2} \left[1 - \frac{(L \pm x)^2}{t} + \frac{(L \pm x)^4}{12t^2} \right]).$$

According to the QSA in the diffusion-controlled limit at large $k \rightarrow \infty$ at times $t \propto k^{-1} \rightarrow 0$, there forms a sharp reaction front $w/|\mathbf{r}_f| \rightarrow 0$ so that in neglect of the reaction front width the solution $s(\mathbf{r}, t)$ defines the the law of its propagation

$$s(\mathbf{r}_f, t) = 0$$

and the evolution of particle distributions $a(\mathbf{r}, t) = s(\mathbf{r}, t) > 0$ within the island and $b(\mathbf{r}, t) = |s(\mathbf{r}, t) < 0|$ beyond it. Considering the domain $x \geq 0$ in view of $x \leftrightarrow -x$ symmetry and assuming that $|x - L| \ll t, L$, from Eqs. (13) and (14) we conclude that at $1 \ll t \ll L^2$, when the diffusion length is much less than the initial distance between the island centers, the ratio $\mathcal{L}_+/\mathcal{L}_-$ is exponentially small ($\mathcal{L}_+/\mathcal{L}_- \sim t e^{-Lx/t}/L$ at $1 \ll t \ll L$ and $\sim e^{-xL/t}$ at $L \ll t \ll L^2$). Therefore, neglecting the contribution of \mathcal{L}_+ and assuming that the radius of a d -dimensional sphere with the center at the point of initial island center $\rho \ll t$, we find from Eqs. (7)–(9)

$$s(\rho, t) + 1 = \frac{(c+1)e^{-\rho^2/4t}}{(\pi t)^{d/2}}(1 - \xi_d),$$

where

$$\xi_d = \frac{(d - \rho^2/2t)}{12t} + \dots$$

Neglecting further the term $\xi_d \ll 1$, we conclude that in agreement with Ref. [37] regardless of the initial island shape (hypercube or hypersphere) at $1 \ll t \ll L^2$ each of the islands takes the shape of a d -dimensional sphere with the front radius $\rho_f(t)$ which changes by the law

$$\rho_f(t) = \sqrt{2dt \ln(t_c/t)}, \quad (16)$$

from which it follows that at any d in the limit of large $c \gg 1$ the island first expands reaching some maximal radius ρ_f^M , and then it contracts disappearing in the collapse point

$$t_c = \frac{(c+1)^{2/d}}{\pi} = \frac{(\gamma N_0)^{2/d}}{4\pi}, \quad (17)$$

where $\gamma = (c+1)/c \approx 1$, N_0 is the initial particle number in the island in units of $h^d b_0$, and at the front turning point $t_M = t_c/e$

$$\rho_f^M = \sqrt{2dt_M} = (\gamma N_0)^{1/d} \sqrt{d/2\pi e}. \quad (18)$$

At large t_c the requirement $\chi_d^f \ll 1$ along with the requirement $t \gg 1$ obviously reduces to the more rigid requirement $t \gg \ln(t_c/t)$. On the other hand, the requirement of ‘‘autonomous’’ death of each of the islands $t_c \ll L^2$ reduces to the requirement

$$\Lambda^{2/d} \ll 1, \quad \Lambda = (c+1)/L^d. \quad (19)$$

III. EVOLUTION OF THE ISLAND-SEA-ISLAND SYSTEM IN THE INSTANTANEOUS SOURCE REGIME

According to Eqs. (13)–(16), at large $L \gg 1$ in the domain $t \gg \text{Max}[1, \ln(t_c/t)]$ evolution of the island bounded by the front becomes independent on its initial size, therefore, the initial distance between the island centers 2ℓ becomes the only length scale determining the evolution. Then, by measuring the length and time in units of ℓ and ℓ^2/D , i.e., going to the dimensionless variables $T = t/L^2$, $X = x/L$, $Y = y/L$, $Z = z/L$, and neglecting the transient terms q_{\pm} , $(v/t)^2 \ll 1$ in Eqs. (13)–(15), we find from Eqs. (7)–(9) and (13)–(15)

$$s + 1 = \frac{2\Lambda}{(\pi T)^{d/2}} \exp\left(-\frac{1 + X^2 + \varrho^2}{4T}\right) \cosh\left(\frac{X}{2T}\right), \quad (20)$$

where $\varrho^2 = Y^2$ or $\varrho^2 = Y^2 + Z^2$ at $d = 2, 3$, respectively. Taking $s_f = 0$ we derive from Eq. (20) the law of the reaction front motion

$$\exp\left(-\frac{1 + X_f^2 + \varrho_f^2}{4T}\right) \cosh\left(\frac{X_f}{2T}\right) = \frac{(\pi T)^{d/2}}{2\Lambda} \quad (21)$$

and we conclude that in the instantaneous source regime evolution dynamics of the island-sea-island system is determined unambiguously by the value of the parameter Λ which in view of the requirement $c \gg 1$ ($\gamma \approx 1$) is the ratio of the initial particle number in the island N_0 to the initial number of sea particles N_{Ω} in the volume $\Omega = (2\ell)^d$:

$$\Lambda = N_0/N_{\Omega}.$$

From Eq. (20) it follows that at any d the points where the concentration of A particles reaches its maximum, which according to Refs. [31,33] we will call the *island centers*, are located on the X axis. Calculating the trajectories of motion of the centers $X_*(T)$ from the condition $\partial s/\partial X = 0$, we obtain from Eq. (20)

$$\tanh\left(\frac{X_*}{2T}\right) = X_*, \quad (22)$$

from which at small $T \ll 1$ we find

$$|X_*| = 1 - 2e^{-|X_*|/T} + \dots, \quad |X_*|/T \gg 1$$

whereas at small $|X_*|/T \ll 1$ we have

$$|X_*| = \sqrt{6(T_s - T)} + \dots, \quad |X_*|/T \ll 1$$

where $T_s = 1/2$. We conclude thus that with increasing T , regardless of the dimension of the system and the value of the parameter Λ , the centers of both islands move toward each other along the universal trajectory (22) from $X_* = \pm 1$ to $|X_*| \rightarrow 0$, merging at $T_s = 1/2$ into the single center $X_* = 0$ in the system center $\mathbf{r} = \mathbf{0}$. It is clear, however, that mutual convergence of the island centers caused by effective

diffusion-controlled “attraction” of the islands continues only until the collapse moment $T_c(\Lambda)$ of each of the islands which depends on the quantity Λ . It is also clear that after expansion and subsequent contraction of the islands, collapse of each of them is completed at the point of the corresponding center

$$X_c = X_*(T_c),$$

the coordinates of which are fixed by the system of equations which follows from Eqs. (21) and (22):

$$\tanh\left(\frac{X_c}{2T_c}\right) = X_c, \tag{23}$$

$$\exp\left(-\frac{1+X_c^2}{4T_c}\right) \cosh\left(\frac{X_c}{2T_c}\right) = \frac{(\pi T_c)^{d/2}}{2\Lambda}. \tag{24}$$

According to Eq. (21), at $T \leq T_s$ on the X axis each of the islands is bounded by two leading front points (by two fronts in the 1D case) $|X_f^-| < |X_*|$ and $|X_f^+| > |X_*|$ which determine the width of the island

$$|X_f^-| < |X_{\text{isl}}| < |X_f^+|$$

and, therefore, the time moment of the island collapse is determined by the condition

$$|X_f^-(T_c)| = |X_f^+(T_c)| = |X_*(T_c)|.$$

With growing Λ the distance to the system center $|X_f^-|$ at the front turning point obviously reduces until at some critical value Λ_* both of the leading front points $\pm X_f^-$ merge in the system center $|X_f^-| = 0$ and, thus, at $\Lambda > \Lambda_*$ coalescence of the islands occurs with the formation of a united island with the half-width $|X_f^+|$. According to Eq. (20), in the system center we find

$$s(\mathbf{0}, T) + 1 = \frac{2\Lambda}{(\pi T)^{d/2}} \exp\left(-\frac{1}{4T}\right) \tag{25}$$

from which it follows immediately that $s(\mathbf{0}, T)$ reaches the maximum $s_M(\mathbf{0}) = \text{Max}_T[s(\mathbf{0}, T)]$ at the time moment

$$T_M = 1/2d$$

from which we find

$$s_M(\mathbf{0}) = 2\Lambda \left(\frac{2d}{\pi e}\right)^{d/2} - 1.$$

Assuming further that $s_M(\mathbf{0}) = 0$ we obtain finally the critical point of coalescence threshold

$$\Lambda_* = \frac{1}{2} \left(\frac{\pi e}{2d}\right)^{d/2} = \begin{cases} 1.03318\dots, & d = 1 \\ 1.06747\dots, & d = 2 \\ 0.84900\dots, & d = 3. \end{cases} \tag{26}$$

Substituting now $T = T_s$ into Eq. (25) and assuming that $s(\mathbf{0}, T_s) = 0$, we find the critical point of threshold of island centers merging

$$\Lambda_s = \frac{\sqrt{e}}{2} \left(\frac{\pi}{2}\right)^{d/2} = \begin{cases} \Lambda_*, & d = 1 \\ 1.29490\dots, & d = 2 \\ 1.62292\dots, & d = 3. \end{cases} \tag{27}$$

above which the formed single-centered island dies in the system center. Indeed, according to Eq. (20), in the system

center we have

$$\partial^2 s / \partial X^2 |_{r=0} = -\frac{\Lambda e^{-1/4T}}{T(\pi T)^{d/2}} (1 - T_s/T)$$

from which, according to Eq. (22), it follows that at the critical point $T_s = \frac{1}{2}$ the transition local minimum of $s \rightarrow$ global maximum of s occurs:

$$s(\mathbf{0}, T < T_s) = \text{Min}_X(s) \rightarrow s(\mathbf{0}, T > T_s) = \text{Max}_X(s).$$

From Eqs. (25)–(27) we conclude that regularities of the island-sea-island system evolution differ qualitatively at $d = 1$ and $d > 1$. In 1D systems $\Lambda_* = \Lambda_s$, that is why in the domain $\Lambda < \Lambda_*$ each of the islands dies individually not touching the partner, whereas above the threshold $\Lambda > \Lambda_*$ the single-centered island formed during coalescence dies in the system center. At $d > 1$ in the range $\Lambda_* < \Lambda < \Lambda_s$ a united (dumbbell-like) two-centered island is formed which again splits into two separated islands (fragmentation) at some moment $T_{fr}(\Lambda)$ with subsequent death in corresponding centers $\pm X_*(T_c)$. It is easy to understand the reasons for absence of the intermediate coalescence-fragmentation domain in 1D systems. Indeed, in 2D and 3D systems the sea always remains topologically continuous (*pathwise connected*), that is why after formation of an isthmus between the islands (coalescence) the current of sea particles normal to the X axis strives to destroy the isthmus ($A + B \rightarrow 0$) and reach this (fragmentation) in the range $\Lambda_* < \Lambda < \Lambda_s$ as the island is depleted. In a qualitative contrast to that, in 1D systems the sea consists of two areas separated by the islands: a finite “internal” sea area enclosed between the fronts $\pm X_f^-$ ($0 \leq |X_{\text{isea}}| < |X_f^-|$) and an unbounded “external” sea $|X_f^+| < |X_{\text{sea}}| < \infty$. Thus, after disappearance of the internal sea area (coalescence) collapse of the formed island in the system center is the only remaining outcome of the reaction in 1D systems.

From Eq. (25) it follows that above the coalescence threshold $\Lambda > \Lambda_*$ the condition $s(\mathbf{0}, T) = 0$ leads to occurrence of two roots $T_0^{(-)} < T_M$ and $T_0^{(+)} > T_M$. The first of these roots, $T_0^{(-)}$, determines the starting time of island coalescence

$$T_0^{(-)} = T_{cl}(\Lambda)$$

and unlimitedly (logarithmically slowly) decreases with an increase in Λ :

$$T_{cl} \propto 1/4 \ln \Lambda, \quad \ln \Lambda \gg 1.$$

The meaning of the second of these roots, $T_0^{(+)}$, depends on system dimension and value of Λ . In 1D systems $T_0^{(+)}$ determines the collapse point of the formed single-centered island

$$T_0^{(+)} = T_c(\Lambda).$$

At $d > 1$ in the range $T_M < T_0^{(+)} < T_s$ ($\Lambda_* < \Lambda < \Lambda_s$) the second root gives the fragmentation point of the two-centered island

$$T_0^{(+)} = T_{fr}(\Lambda),$$

whereas at $T_0^{(+)} > T_s$ it determines the collapse time of the single-centered island which increases unlimitedly with

growing Λ :

$$T_c \propto (2\Lambda)^{2/d}/\pi, \quad \Lambda^{2/d} \gg 1.$$

It is important to note that in the limit of large $\Lambda^{2/d} \gg 1$ at $T \gg \text{Max}[\ln(T_c/T), 1]$ the term $\cosh(X_f/2T) \approx 1$ in Eq. (21) can be neglected, therefore, in the course of evolution the island takes the shape of a d -dimensional sphere, the radius of which [just as in the autonomous evolution domain $\Lambda^{2/d} \ll 1$ (Eq. (16))] changes by the law

$$|X_f^+| = \sqrt{X_f^2 + \varrho_f^2} \approx \sqrt{2dT \ln(T_c/T)}, \quad (28)$$

where

$$T_c = \frac{(2\Lambda)^{2/d}}{\pi} (1 - c_d/\Lambda^{2/d} + \dots) \approx (2\Lambda)^{2/d}/\pi$$

(with $c_d = \pi/2^{(d+2)/d}d$) instead of $T_c = (\Lambda^{2/d})/\pi$ in the domain of autonomous evolution. This result is a trivial consequence of the fact that in the limit of large T , when diffusion length becomes much larger than the initial distance between the islands, the evolution of the island formed during coalescence should obey asymptotically the law of evolution from an instantaneous source with the twice initial number of particles $2N_0$. According to Eq. (20), in 2D and 3D systems the half-width (radius) of the isthmus between the islands in the section $X = 0$ grows during coalescence by the law

$$|\varrho_{0f}| = \sqrt{4T \ln[2\Lambda/(\pi T)^{d/2}] - 1}$$

reaching the maximum

$$|\varrho_{0f}^M| = \sqrt{(\Lambda/\Lambda_*)^{2/d} - 1}$$

at the time moment

$$T_M^e = (\Lambda/\Lambda_*)^{2/d}/2d$$

from which in the upper limit of the fragmentation domain $\Lambda = \Lambda_s$ we obtain

$$T_M^e(\Lambda_s)/T_s = e^{(1-d)/d} = \begin{cases} 0.60653\dots, & d = 2 \\ 0.51341\dots, & d = 3 \end{cases}$$

and

$$|\varrho_{0f}^M(\Lambda_s)| = \sqrt{de^{(1-d)/d} - 1} = \begin{cases} 0.46158\dots, & d = 2 \\ 0.73501\dots, & d = 3. \end{cases}$$

Correspondingly, in the limit of large $\Lambda^{2/d} \gg 1$ under expansion and subsequent contraction of the d -dimensional sphere in accord with Eq. (28) we find $T_M^e(\Lambda \rightarrow \infty)/T_c = 1/e$ and $|\varrho_{0f}^M(\Lambda \rightarrow \infty)| = (\Lambda/\Lambda_*)^{1/d}$ at the front turning point. Figure 1 demonstrates the dependencies $T_c(\Lambda)$, $T_{cl}(\Lambda)$, and $T_{fr}(\Lambda)$ calculated from Eqs. (23)–(25) for $d = 1, 2, 3$. These dependencies reveal a comprehensive picture of location and extension of the domains of autonomous death of the islands (I), individual death of the islands below the coalescence threshold (II), coalescence-fragmentation of the two-centered island with subsequent individual death of each of the islands

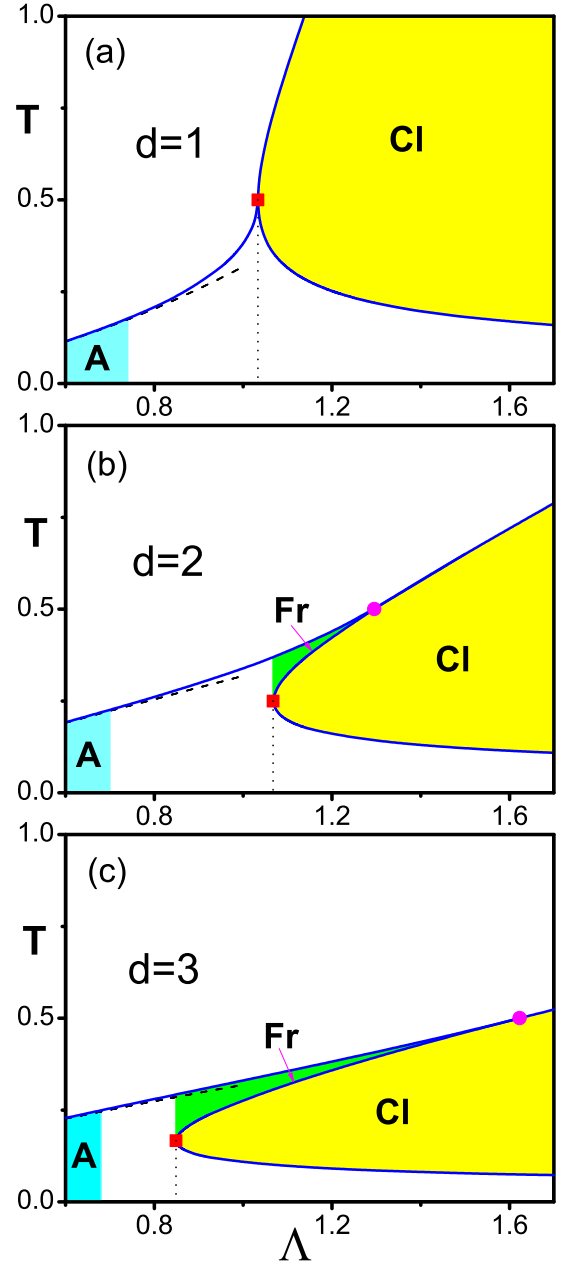


FIG. 1. Dependencies $T_c(\Lambda)$, $T_{cl}(\Lambda)$, and $T_{fr}(\Lambda)$ calculated from Eqs. (23)–(25) for $d = 1$ (a), $d = 2$ (b), and $d = 3$ (c). The areas of autonomous collapse, coalescence, and fragmentation are colored. The critical points (Λ_*, T_M) and (Λ_s, T_s) are marked by square and circle, respectively. The dashed lines show the asymptotics of the autonomous collapse [Eq. (16)].

(III), and coalescence-collapse of the single-centered island in the system center (IV).

IV. EVOLUTION OF FRONT TRAJECTORIES

Figures 2–4 show the dependencies $|X_f^-(T)|$, $|X_f^+(T)|$, and $|X_*(T)|$ calculated from Eqs. (7)–(12) ($L = 10^2$, $v = 0$) and Eqs. (21) and (22) ($\varrho = 0$) for $d = 1, 2$, and 3 , respectively. These dependencies, in combination with the behavior of the velocities along trajectories, demonstrate the

key features of evolution of trajectories of fronts and of island centers with growing parameter Λ .

A. 1D systems

From Fig. 2 it is seen that in 1D systems with increasing Λ the mutual “self-accelerating” convergence of the island centers is accompanied by the corresponding asymmetric “deformation” of the front trajectories.

(a) *The trajectory $|X_f^-(T)|$.* In the domain $\Lambda < \Lambda_a^- \approx 0.982\Lambda_*$ the velocity of front motion $|V_f^-| = |dX_f^-/dT|$ along the trajectory $|X_f^-|$ decreases monotonically up to the front turning point $V_f^- = 0$ after the passage of which both of the fronts $|X_f^\pm|$ move toward each other accelerating up to the point of island collapse $|V_f^\pm(T \rightarrow T_c)| \rightarrow \infty$. At $\Lambda_a^- < \Lambda < \Lambda_*$ on the trajectory $|X_f^-(T)|$ two inflection points, $\text{Min}|V_f^-|$ and $\text{Max}|V_f^-|$, arise between which the domain of front acceleration appears and expands. As Λ approaches Λ_* , the amplitude of $\text{Max}|V_f^-|$ increases unlimitedly $\text{Max}|V_f^-|(\Lambda \rightarrow \Lambda_*) \rightarrow \infty$ decreasing abruptly to 0 at the front turning point with subsequent rapid collapse of the island. The reason for this behavior is obviously the competition between two opposing trends: (i) the striving of each of the islands to “destroy” the finite (internal) sea area as motion of the front $|X_f^-|$ accelerates and (ii) the striving of the unlimited sea area to “destroy” the island as motion of the front $|X_f^+|$ accelerates. At the stage of accelerating motion of the front $|X_f^-|$ the process (i) is dominant, whereas after passage of the point $\text{Max}|V_f^-|$ the process (ii) wins the competition. It is remarkable that precisely at the critical point Λ_* both of the islands and the internal sea area die *simultaneously* at the time moment $T = T_s$: $|X_f^\pm| \rightarrow 0$, $|V_f^\pm| \rightarrow \infty$ as $T \rightarrow T_s$. In the domain of coalescence $\Lambda > \Lambda_*$, the process (i) wins the competition, that is why the front velocity grows unlimitedly up to the coalescence point: $|X_f^-| \rightarrow 0$, $|V_f^-| \rightarrow \infty$ as $T \rightarrow T_{cl}$.

(b) *The trajectory $|X_f^+(T)|$.* In the domain of individual island collapse $\Lambda < \Lambda_*$, after passage of the front turning point $V_f^+ = 0$ the front velocity monotonically increases unlimitedly everywhere up to the point of island collapse T_c : $|V_f^+| \rightarrow \infty$ as $T \rightarrow T_c < T_s$. At $\Lambda > \Lambda_*$ two inflection points, $\text{Max}|V_f^+|$ and $\text{Min}|V_f^+|$, arise on the trajectory $|X_f^+|$ between which the domain of front motion deceleration appears and expands. With an increase in Λ , the amplitude of ratio $\text{Max}|V_f^+|/\text{Min}|V_f^+|$ decreases rapidly, so at large $\Lambda \gg \Lambda_*$ the domain of front deceleration actually disappears. Since the domain of front deceleration arises in the vicinity $T \approx T_s < T_c$, it is qualitatively clear that the reason for front motion deceleration is a rapid increase in the concentration of island particles in the system center against a background of merging of the island centers in a united center at $T = T_s = T_M$ where the concentration reaches the maximum. According to Fig. 2, with increasing Λ , by the time moment $T \approx T_s$ the distance from the front to the system center rapidly increases and, as a consequence, the effect of passage through the maximum in the system center on front motion decreases up to complete disappearance at large Λ .

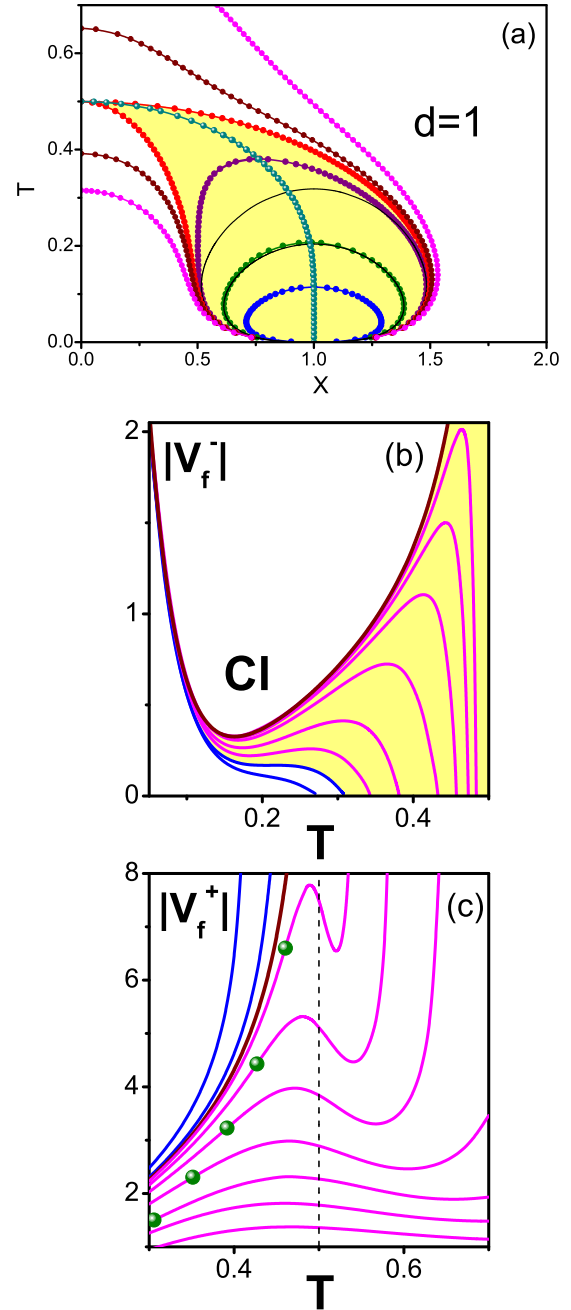


FIG. 2. 1D systems: (a) The trajectories $|X_f^+(T)|$ and $|X_f^-(T)|$ calculated for $\Lambda = 0.6, 0.8, 1$, $\Lambda_* = 1.03318, 1.05$, and 1.1 according to Eqs. (7)–(12) ($L = 10^2$, $v = 0$) (filled circles) and Eq. (21) ($\varrho = 0$) (thick lines). In accordance with Fig. 1(a) the growth of Λ corresponds to the visually observed growth of T_c . The area of individual collapse below the coalescence threshold is colored. Semifilled circles show the trajectory of the island center $|X_s(T)|$ [Eq. (22)]. The trajectories of autonomous collapse calculated from Eq. (16) for $\Lambda = 0.6, 0.8$, and 1 are shown by thin lines. (b) Time dependencies $|V_f^-(T)|$ up to the turning point calculated from Eq. (21) for $\Lambda = 1.01, 1.015, 1.02, 1.025, 1.03, 1.032, 1.0325, 1.033$, and Λ_* (from bottom to top). The area with two inflection points is colored. (c) Time dependencies $|V_f^+(T)|$ calculated from Eq. (21) for $\Lambda = 1.02, 1.03, \Lambda_*, 1.035, 1.04, 1.05, 1.07, 1.11, 1.14$, and 1.2 (from top to bottom). The circles mark the starting points of coalescence.

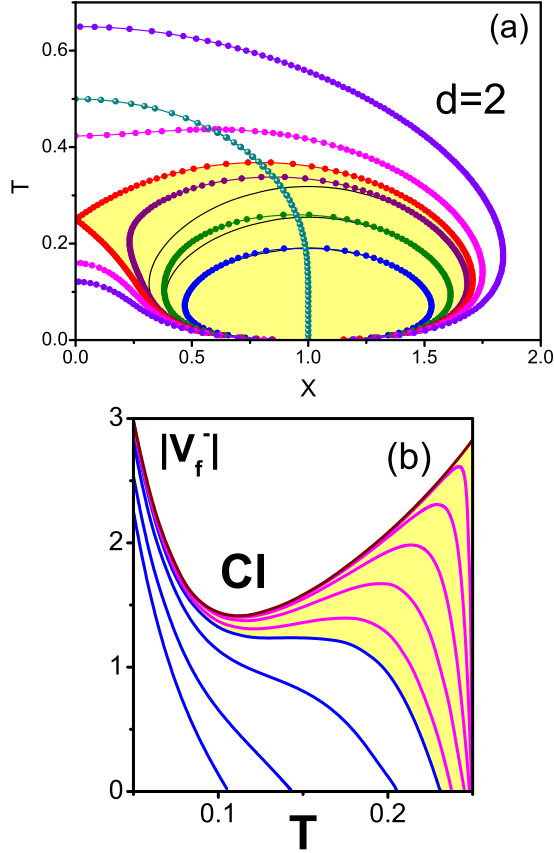


FIG. 3. 2D systems: (a) The trajectories $|X_f^+(T)|$ and $|X_f^-(T)|$ calculated for $\Lambda = 0.6, 0.8, 1, \Lambda_* = 1.06747, 1.2,$ and 1.5 according to Eqs. (7)–(12) ($L = 10^2, v = 0$) (filled circles) and Eq. (21) ($\varrho = 0$) (thick lines). In accordance with Fig. 1(b) the growth of Λ corresponds to the visually observed growth of T_c . The area of individual collapse below the coalescence threshold is colored. Semifilled circles show the trajectory of the island center $|X_*(T)|$ [Eq. (22)]. The trajectories of autonomous collapse calculated from Eq. (16) for $\Lambda = 0.6, 0.8,$ and 1 are shown by thin lines. (b) Time dependencies $|V_f^-(T)|$ up to the turning point calculated from Eq. (21) for $\Lambda = 0.08, 0.09, 1, 1.04, 1.05, 1.06, 1.065, 1.067, 1.06744,$ and Λ_* (from bottom to top). The area with two inflection points is colored.

B. 2D and 3D systems

From Fig. 3 it is seen that in the 2D case, as well as in the 1D case, at $\Lambda > \Lambda_a^- \approx 0.974\Lambda_*$ two inflection points, $\text{Min}|V_f^-|$ and $\text{Max}|V_f^-|$, arise on the trajectory $|X_f^-(T)|$ between which the domain of front acceleration appears and expands. In a qualitative contrast to 1D systems, however, as Λ approaches Λ_* , the amplitude of $\text{Max}|V_f^-|$ approaches the finite value $|V_{f*}^-|$ which is reached precisely at the critical point $\Lambda = \Lambda_*$ where $|X_f^-| \rightarrow 0, |V_f^-| \rightarrow |V_{f*}^-|$ as $T \rightarrow T_M$. Moreover, at $\Lambda = \Lambda_*$ at the time moment $T = T_M$ “elastic” reflection of the front from the system center occurs with a sudden reversal of velocity sign:

$$\pm|V_f^-|(T = T_M - 0) \rightarrow \mp|V_f^-|(T = T_M + 0).$$

In the coalescence-fragmentation domain $\Lambda_* < \Lambda < \Lambda_s$ the front $|X_f^-|$, moving to the system center, disappears at

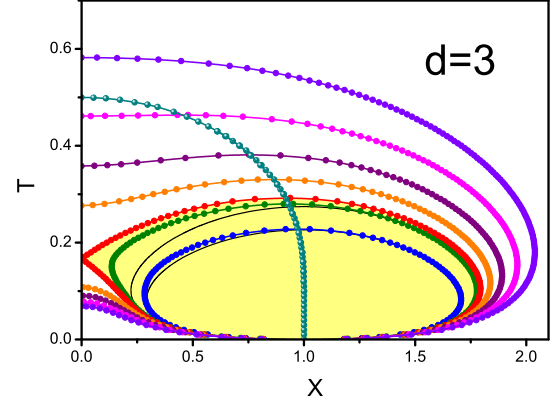


FIG. 4. 3D systems: The trajectories $|X_f^+(T)|$ and $|X_f^-(T)|$ calculated for $\Lambda = 0.6, 0.8, \Lambda_* = 0.84900, 1, 1.2, 1.5,$ and 1.9 according to Eqs. (7)–(12) ($L = 10^2, v = 0$) (filled circles) and Eq. (21) ($\varrho = 0$) (thick lines). In accordance with Fig. 1(c) the growth of Λ corresponds to the visually observed growth of T_c . The area of individual collapse below the coalescence threshold is colored. Semifilled circles show the trajectory of the island center $|X_*(T)|$ [Eq. (22)]. The trajectories of autonomous collapse calculated from Eq. (16) for $\Lambda = 0.6$ and 0.8 are shown by thin lines.

the coalescence point ($|X_f^-| \rightarrow 0, |V_f^-| \rightarrow \infty$ as $T \rightarrow T_{cl} < T_M$), and arises again at the fragmentation point ($|X_f^-| \rightarrow 0, |V_f^-| \rightarrow \infty$ as $T \rightarrow T_{fr} < T_s$), moving to the island center, with its subsequent collapse at the point T_c . In a qualitative contrast to 1D systems, after passage of the turning point $|V_f^+| = 0$, the front $|X_f^+|$ moves with an unlimitedly increasing velocity at any Λ up to the collapse point $|X_f^+| \rightarrow |X_c|, |V_f^+| \rightarrow \infty$ as $T \rightarrow T_c$. 3D systems demonstrate the similar behavior (Fig. 4) with $\Lambda_a^- \approx 0.957\Lambda_*$.

C. Front trajectories in the vicinity of coalescence, fragmentation, and collapse points $X_f^\pm \rightarrow 0$

From Eq. (21) we find that in the limit $X_f^\pm \rightarrow 0$ (in view of $X \leftrightarrow -X$ symmetry we shall assume that $X \geq 0$)

$$V_f X_f = \frac{d(1 - T_M/T + \epsilon_M)}{(T_s/T - 1 + \epsilon_s)}, \quad (29)$$

where

$$\epsilon_M = X_f^2 T_M (1/T - 1)/T - s(\mathbf{0}, T) + \dots,$$

$$\epsilon_s = -X_f^2 (1 - 1/T + 1/12T^2)/4T^2 + \dots,$$

and $\epsilon_{M,s} \rightarrow 0$ as $|T - T_0|, X_f \rightarrow 0$ where $T_0(\Lambda) = T_0^{(-)}(\Lambda) = T_{cl}$ or $T_0(\Lambda) = T_0^{(+)}(\Lambda) = T_{fr}, T_c$. Assuming further that $T_0 \neq T_M, T_s$ in the limit $|T - T_0| \rightarrow 0$, we obtain from Eq. (29)

$$X_f = \sqrt{2dD(T_0 - T)}$$

and

$$V_f = -\text{sgn}(D) \sqrt{\frac{dD}{2(T_0 - T)}}, \quad (30)$$

where

$$D = \frac{T_M - T_0}{T_s - T_0}.$$

From Eq. (30) it follows that at $\Lambda > \Lambda_*$ in 1D systems ($T_M = T_s = \frac{1}{2}$) the fronts of collapse $X_f^+(T_0 = T_c > T_M)$ and coalescence $X_f^-(T_0 = T_{cl} < T_M)$ reach the system center with the same reduced velocity *regardless* of Λ :

$$\mathcal{V}_f = |V_f| \sqrt{|T_0 - T|} = 1/\sqrt{2}.$$

In 2D and 3D systems, behavior of the fronts changes qualitatively. With an increase in Λ , the reduced velocities of coalescence and fragmentation fronts increase from $\mathcal{V}_f \rightarrow 0$ at $\Lambda \rightarrow \Lambda_* + 0$ to $\mathcal{V}_f = 1/\sqrt{2}$ at $\Lambda \gg \Lambda_*$ and to $\mathcal{V}_f \rightarrow \infty$ at $\Lambda \rightarrow \Lambda_s - 0$, respectively. In its turn, with increasing Λ the reduced velocity of collapse of the single-centered island ($\Lambda > \Lambda_s$) decreases from $\mathcal{V}_f \rightarrow \infty$ at $\Lambda \rightarrow \Lambda_s + 0$ to the constant $\mathcal{V}_f = \sqrt{d}/2$ at $\Lambda \gg \Lambda_s$. It is clear that ‘‘abnormal’’ deceleration $\mathcal{V}_f(T_0 \rightarrow T_M) \rightarrow 0$ and acceleration $\mathcal{V}_f(T_0 \rightarrow T_s) \rightarrow \infty$ of front motion in the vicinity of the critical points Λ_* and Λ_s , respectively, relate to a radical change in the laws of front motion at these points. The detailed analysis which will be presented below shows that at the critical point $\Lambda = \Lambda_*$ ($T_0 = T_M$) the fronts of coalescence ($T \rightarrow T_M - 0$) and fragmentation ($T \rightarrow T_M + 0$) move by the law of ‘‘elastic’’ front reflection

$$X_f^\pm = \pm(T_M - T)\sqrt{2d^2/(d-1)}. \quad (31)$$

At the critical point of merging of the centers $\Lambda = \Lambda_s$ we find

$$X_f^\pm = [12(d-1)(T_s - T)]^{1/4}. \quad (32)$$

As we shall see below, the first of these results is a direct consequence of rapid $\propto (T_M - T)^2$ disappearance of sea particles in the system center and as a rapid increase in their concentration after reflection of the front. The second of these results [which is easily derived from (29)] is a direct consequence of formation of a superellipse (2D) or superellipsoid (3D) at the final stage of island collapse. To complete the picture, we shall also indicate the law of front motion at the critical point $\Lambda = \Lambda_* = \Lambda_s$ for the 1D case:

$$X_f^\pm = \sqrt{2(3 \pm \sqrt{6})(T_M - T)}. \quad (33)$$

V. EVOLUTION OF ISLANDS IN THE VICINITY OF COALESCENCE, FRAGMENTATION, AND COLLAPSE POINTS

In the previous section we focused on front trajectories along the X axis, $X_f^\pm(\Lambda, T)|_{\varrho_f=0}$, which determine the evolution of width of the islands and the key features of their coalescence, fragmentation, and collapse. In 1D systems these trajectories provide comprehensive information on evolution of islands, whereas in 2D and 3D systems the description of shape evolution of the islands $\varrho_f(\Lambda, T) = \mathcal{F}[X_f(\Lambda, T)]$ is necessary for a complete picture of their evolution. In this section, our goal is a detailed analysis of the evolution of shape of the islands in the vicinity of their coalescence, fragmentation, and collapse points.

Assuming that $|X|/T, X^2/T \ll 1$ and $\varrho^2/T \ll 1$ we find from Eq. (20)

$$s + 1 = \frac{2\Lambda e^{-1/4T}}{(\pi T)^{d/2}} \left(1 - \frac{X^2}{4T} \mathcal{P}_2 + \frac{X^4}{T^2} \mathcal{P}_4 - \frac{\varrho^2}{4T} + \dots \right), \quad (34)$$

where

$$\mathcal{P}_2(T) = 1 - 1/2T$$

and

$$\mathcal{P}_4(T) = (1 - 1/T + 1/12T^2)/32.$$

Let now as before $s(\mathbf{0}, T_0) = 0$ where, depending on the value of Λ , the time moment T_0 is the point of coalescence T_{cl} , fragmentation T_{fr} , or collapse of the single-centered island T_c . Then, introducing the reduced time $\mathcal{T} = (T_0 - T)/T_0$ in the limit of small $|\mathcal{T}| \ll 1$ we obtain from Eq. (34)

$$s = s(\mathbf{0}, T) - \frac{X^2}{4T_0} \mathcal{P}_2^0 + \frac{X^4}{T^2} \mathcal{P}_4 - \frac{\varrho^2}{4T} + \dots, \quad (35)$$

where

$$\mathcal{P}_2^0 = (1 - T_s/T_0)(1 + s(\mathbf{0}, T)) + \mathcal{T}(1 - 1/T_0) + \dots,$$

$$s(\mathbf{0}, T) = \mathcal{T}d(1 - T_M/T_0)/2 + m\mathcal{T}^2 + \dots,$$

and

$$m = \frac{(d+2)}{8}(d - 1/T_0) + 1/32T_0^2.$$

Assuming further that $s_f = 0$ we derive from Eq. (35)

$$s(\mathbf{0}, T) = \frac{X_f^2}{4T_0} \mathcal{P}_2^0 - \frac{X_f^4}{T^2} \mathcal{P}_4 + \frac{\varrho_f^2}{4T} + \dots. \quad (36)$$

A. Self-similar evolution of islands at the final collapse stage at $\Lambda \geq \Lambda_s$

1. Self-similar collapse at the critical point $\Lambda_s = \Lambda_*$ of 1D systems

At the critical point $\Lambda = \Lambda_s$ we have $T_0 = T_s = T_c = \frac{1}{2}$ from which it follows

$$\mathcal{P}_2^0 = -\mathcal{T} + \dots,$$

$$s(\mathbf{0}, \mathcal{T}) = \mathcal{T}(d-1)/2 + (d^2-3)\mathcal{T}^2/8 + \dots,$$

and we derive from Eq. (36)

$$s(\mathbf{0}, \mathcal{T}) = -X_f^2\mathcal{T}/2 + X_f^4/12 + \rho_f^2/2 + \dots. \quad (37)$$

In the 1D case, where $\Lambda_s = \Lambda_*$, $T_s = T_M$, and $\varrho = 0$, from Eq. (37) we reproduce immediately the result of (33):

$$X_f^\pm = \sqrt{(3 \pm \sqrt{6})\mathcal{T}}.$$

From Eq. (35) a remarkable fact follows that in 1D systems at the final collapse stage the distribution of particles in the island and internal area of the sea takes the universal scaling form

$$s(X, \mathcal{T}) = \mathcal{T}^2 \Phi(|X|/\sqrt{\mathcal{T}}). \quad (38)$$

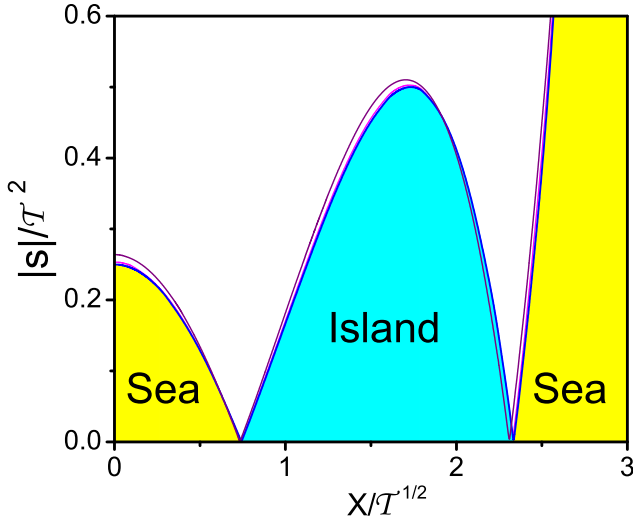


FIG. 5. Collapse of the normalized distribution of particles $|s(X/\sqrt{T})|/T^2$ to the scaling function (38) at $\Lambda = \Lambda_*$. Thin lines: $T = 0.04, 0.01$; thick line: $T \rightarrow 0$ [Eq. (20)]. The areas under scaling function $\Phi(|X|/\sqrt{T})$ are colored.

As a consequence of this fact, we conclude that at the critical point $\Lambda_s = \Lambda_*$ at the final collapse stage the ratio of island width $X_f^+ - X_f^-$ to the half-width of the internal sea area X_f^- ,

$$g_{1/s} = \frac{X_f^+ - X_f^-}{X_f^-} = \sqrt{\frac{3 + \sqrt{6}}{3 - \sqrt{6}}} - 1 = 2.14626,$$

and the ratio of front to center widths $|X_f^\pm - X_\star|$ [where, according to Eq. (22), $X_\star = \sqrt{3T}$]

$$g_\pm = \frac{X_f^\pm - X_\star}{X_\star - X_f^\mp} = \frac{\sqrt{3 + \sqrt{6}} - \sqrt{3}}{\sqrt{3} - \sqrt{3 - \sqrt{6}}} = 0.60839\dots$$

remain constant up to the collapse point. According to Eq. (38), in the scaling regime the number of island particles should decrease by the law $\mathcal{N} \propto T^{5/2}$. The exact calculation from Eq. (35) gives

$$\mathcal{N}/\mathcal{N}_0 = m_1 T^{5/2},$$

where $m_1 = 0.24312\dots$. Calculating further the ratio of particle number on the half-width of the internal sea area to particle number in the island we obtain $\mathcal{N}_{\text{isea}}/\mathcal{N} = 0.24118\dots$ from which it follows that at the final collapse stage the majority of island particles, $\approx \frac{3}{4}$, die in the “external” front X_f^+ , whereas only $\approx \frac{1}{4}$ of island particles die in the “internal” front X_f^- . From Fig. 5 it is seen that the calculated from Eq. (20) normalized particle distribution $s(X/\sqrt{T})/T^2$ converges to scaling function (38) at $T \approx < 0.04$ from which we conclude that $\sim 10^{-4}$ of the initial number of particles die in the scaling regime (38).

2. Final stage of collapse at the critical point Λ_s of 2D and 3D systems

In a radical contrast to 1D systems, where at the critical point of merging of the centers $T_s = \frac{1}{2}$ both of the islands disappear at the moment of island contact $[X_f^+(T_s) = X_f^-(T_s) =$

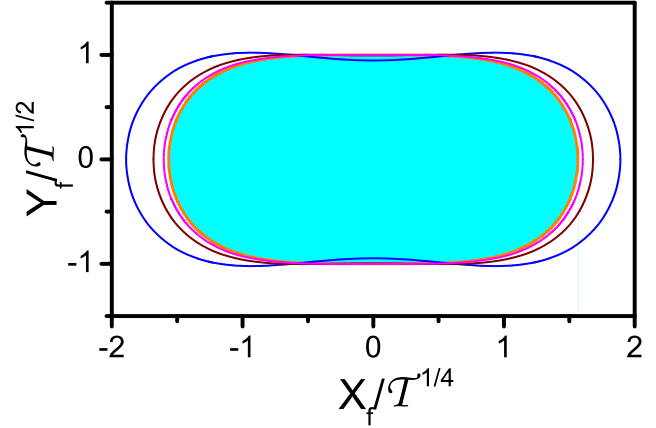


FIG. 6. Final stage of 2D island evolution at the critical point $\Lambda = \Lambda_s$: collapse of island shape to the superellipse in the scaling coordinates $Y_f/T^{1/2}$ vs $X_f/T^{1/4}$. Thin lines: $T = 0.1, 0.01$, and 0.001 [Eq. (21)]; thick line: Eq. (39). The area of superellipse is colored.

0], in 2D and 3D systems long before island collapse a united two-centered island is formed ($T_{cl} < T_M < T_s$) which disappears at the point of merging of the centers $[X_f^+(T_s) = 0]$. From Eq. (37) it follows that at $d > 1$, at the final collapse stage $T \ll 1$, the two-centered dumbbell-like island takes the shape of a superellipse (2D) or superellipsoid (3D):

$$\left(\frac{X_f}{X_f^m}\right)^4 + \left(\frac{\varrho_f}{\varrho_f^m}\right)^2 = 1, \quad (39)$$

where, according to Eq. (32), the major semiaxis of the superellipse (superellipsoid) contracts by the law

$$X_f^m(T) = X_f^+(T) = [6(d-1)T]^{1/4},$$

whereas its minor semiaxis contracts by the law

$$\varrho_f^m(T) = [(d-1)T]^{1/2}$$

and, therefore, the aspect ratio of the superellipse (superellipsoid) contracts by the law

$$\mathcal{A} = \frac{\varrho_f^m}{X_f^m} = \left[\frac{(d-1)T}{6}\right]^{1/4} \rightarrow 0$$

as $T \rightarrow 0$. Thus, we conclude that in 2D and 3D systems at the critical point Λ_s the island asymptotically takes the shape of a quasi-one-dimensional “string,” the length of which contracts unlimitedly by the law $\propto T^{1/4}$ as $T \rightarrow 0$. From Eq. (35) it follows that at the final collapse stage distribution of particles in the island takes the universal scaling form

$$s = T \mathcal{F}_d\left(\frac{|X|}{T^{1/4}}, \frac{|\varrho|}{T^{1/2}}\right), \quad (40)$$

from which, taking into account Eq. (39), for the number of particles in the island we obtain

$$\mathcal{N}/2\mathcal{N}_0 = m_d T^{(2d+3)/4},$$

where $m_2 = 0.15091\dots$ and $m_3 = 0.32025\dots$. Figure 6 presents the calculated from Eq. (21) evolution of front at the final stage of 2D island collapse in the scaling coordinates

$Y_f/\mathcal{T}^{1/2}$ vs $X_f/\mathcal{T}^{1/4}$. It is seen that the shape of the island converges to superellipse (39) at $\mathcal{T} < \sim 10^{-3}$. The same picture is observed in the 3D case from which we conclude that $\sim 10^{-6}$ (2D) and $\sim 10^{-7}$ (3D) of the initial number of particles, respectively, die in the scaling regime (40).

3. Final stage of collapse of single-centered island ($\Lambda > \Lambda_s$)

In agreement with Eq. (30), from Eq. (36) at $\chi = T_s/T_c < 1$ in the limit of small $\mathcal{T} \rightarrow 0$ we asymptotically find

$$X_f^+ = \sqrt{\frac{(d-\chi)\mathcal{T}}{\chi(1-\chi)}}(1 + \mu\mathcal{T} + \dots), \quad (41)$$

where at $1 - \chi \ll 1$ coefficient $|\mu| \propto (d - \chi)/(1 - \chi)^2$ from which it follows that in 1D systems the crossover $\mathcal{T}^{1/2} \rightarrow \mathcal{T}^{1/2}$ to asymptotics (41) is realized at $\mathcal{T} \ll (1 - \chi)$, whereas in 2D and 3D systems the crossover $\mathcal{T}^{1/4} \rightarrow \mathcal{T}^{1/2}$ to asymptotics (41) is realized at $\mathcal{T} \ll (1 - \chi)^2$. From Eq. (36) we conclude thus that in 2D and 3D systems at the final collapse stage $\mathcal{T} \ll (1 - \chi)^2$, the single-centered island takes at any $\Lambda > \Lambda_s$ the shape of an ellipse (2D) or ellipsoid of revolution (3D):

$$\left(\frac{X_f}{X_f^m}\right)^2 + \left(\frac{\varrho_f}{\varrho_f^m}\right)^2 = 1, \quad (42)$$

where the major semiaxis of the ellipse (ellipsoid) contracts by the law

$$X_f^m = X_f^+ = \sqrt{\frac{(d-\chi)\mathcal{T}}{\chi(1-\chi)}},$$

whereas its minor semiaxis contracts by the law

$$\varrho_f^m = \sqrt{(d-\chi)\mathcal{T}/\chi}$$

so that asymptotically the island contracts *self-similarly* with the constant aspect ratio

$$\mathcal{A} = \varrho_f^m/X_f^m = \sqrt{1-\chi}.$$

As expected, in the limit $\chi \rightarrow 1$ ($\Lambda \rightarrow \Lambda_s$), the island inherits asymptotically the shape of a quasi-1D “string,” $\mathcal{A}(\chi \rightarrow 1) \rightarrow 0$, whereas according to Eq. (28) in the opposite limit $\chi \ll 1$ ($\Lambda/\Lambda_s \gg 1$) the island contracts in the shape of a d -dimensional sphere $\mathcal{A}(\chi \rightarrow 0) \rightarrow 1$. According to Eqs. (35) and (42) for asymptotics of the particle number in the island we find

$$\mathcal{N}/2\mathcal{N}_0 = q_d(\Lambda)\mathcal{T}^{(d+2)/2}, \quad (43)$$

where

$$q_d(\Lambda) = \frac{\alpha_d(d-\chi)^{(d+2)/2}}{\Lambda\chi^{d/2}\sqrt{1-\chi}}$$

and $\alpha_1 = 1/6$, $\alpha_2 = \pi/32$, $\alpha_3 = \pi/60$. From Eq. (43) it follows that in the vicinity of the critical point $1 - \chi \ll 1$ by the time of crossover to asymptotics (41) $\propto (1 - \chi)^{(2d+3)/2}$ of the initial number of particles remain in the d -dimensional island. With growing Λ , the coefficient $q_1(\Lambda)$ increases rapidly, and the coefficients $q_{2,3}(\Lambda)$ decrease rapidly reaching the values of $q_1(\infty) = \sqrt{2/\pi}/3$, $q_2(\infty) = \frac{1}{2}$, and $q_3(\infty) = 3\sqrt{6/\pi}/5$ known for a d -dimensional sphere [37].

B. Evolution of 2D and 3D islands in the vicinity of coalescence and fragmentation points ($\Lambda \geq \Lambda_*$)

1. Shape of islands at the starting points of coalescence T_{cl} and fragmentation T_{fr}

Let now $\chi_s = T_s/T_0 > 1$ where T_0 is the starting point of coalescence ($\chi_s > d$) or fragmentation ($1 < \chi_s < d$) of the islands $s(\mathbf{0}, T_0) = 0$. Then, according to Eq. (35), we find that at the point $T = T_0$ ($\mathcal{T} = 0$) of contact of the islands $X_f^-(T_0) = 0$ in the vicinity $X_f \ll \min(\sqrt{\chi_s - 1}, T_0)$ of the system center the front of each of the islands takes the form of an angle (2D) or cone of revolution (3D) with a vertex in the system center $\mathbf{r} = \mathbf{0}$ and the χ_s -dependent value of opening angle 2θ where

$$\tan \theta = |\varrho_f|/X_f = \sqrt{\chi_s - 1}. \quad (44)$$

From Eq. (44) it follows that in the coalescence domain ($T_{cl} < T_M$) the angle $\theta_{cl}(\Lambda)$ increases from $\theta_{cl}(\Lambda_*) = \pi/4$ (2D) or $\tan^{-1}\sqrt{2}$ (3D) to $\theta_{cl}(\infty) = \pi/2$ with an increase in Λ , whereas in the fragmentation domain ($T_M < T_{fr} < T_s$) the angle $\theta_{fr}(\Lambda)$ decreases from $\theta_{fr}(\Lambda_*) = \theta_{cl}(\Lambda_*)$ to $\theta_{fr}(\Lambda \rightarrow \Lambda_s) \rightarrow 0$ with an increase in Λ . We conclude thus that, as expected, (a) at any $\Lambda_* < \Lambda < \Lambda_s$ the angle of coalescence is always greater than that of fragmentation

$$\theta_{cl}(\Lambda) > \theta_{fr}(\Lambda),$$

and (b) in the limit $\Lambda \rightarrow \Lambda_s$ ($\chi_s \rightarrow 1$) at the moment of start of fragmentation T_{fr} both of the islands “inherit” the shape of a quasi-1D string $|\varrho_f|/X_f \rightarrow 0$. According to Eq. (35), in this limit the distribution of particles in each of the islands is determined by the expression

$$s = (\chi_s - 1)X^2/2 - X^4/12 - \varrho^2/2 + \dots$$

from which at the point of fragmentation T_{fr} the island width is

$$X_f^+ = \sqrt{6(\chi_s - 1)},$$

the coordinate of the island center is $X_* = X_f^+/\sqrt{2}$, the concentration of A particles in the island center is $s_* = 3(\chi_s - 1)^2/4$, the amplitude $|\varrho_{f*}|$ in the island center is $|\varrho_{f*}| = \sqrt{3/2}(\chi_s - 1)$ so that $|\varrho_{f*}|/X_f^+ = \sqrt{\chi_s - 1}/2$, and the fraction of particles remaining in each of the islands is $\mathcal{N}/\mathcal{N}_0 \propto (\chi_s - 1)^{(2d+3)/2}$. As an illustration, Fig. 7 presents the sequential stages of coalescence, fragmentation, and collapse of 2D islands for $\Lambda = 1.2$, which demonstrate the key features of the evolution of their shape in the range $\Lambda_* < \Lambda < \Lambda_s$.

2. Elastic reflection of the front at the critical point $\Lambda = \Lambda_*$

According to Eq. (35), at the critical point $\Lambda = \Lambda_*$ ($T_0 = T_M$) we find $s(\mathbf{0}, |\mathcal{T}|) = -d\mathcal{T}^2/4 + \dots$, $\mathcal{P}_2^0 = (1 - d) + \dots$, and conclude that at $|\mathcal{T}|$, $X_f \ll 1$ the front of each of the islands takes the shape of a hyperbola (2D) or hyperboloid of revolution (3D)

$$\left(\frac{X_f}{X_f^m}\right)^2 - \left(\frac{\varrho_f}{\varrho_f^m}\right)^2 = 1, \quad (45)$$

where real, $X_f^m = X_f^-$, and imaginary, ϱ_f^m , semiaxes of the hyperbola (hyperboloid) first contract ($\mathcal{T} > 0$), and then grow

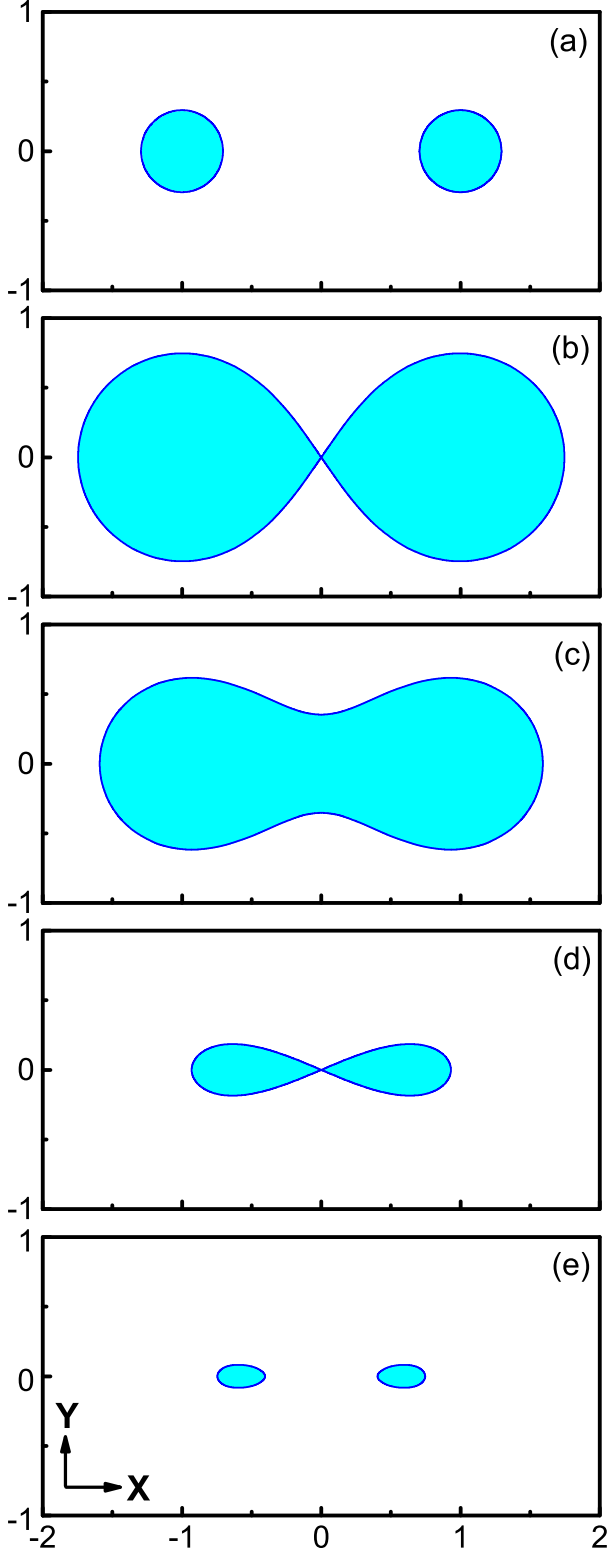


FIG. 7. Sequential stages of coalescence, fragmentation, and collapse of 2D islands calculated from Eq. (21) at $\Lambda = 1.2$ ($T_c = 0.4368$) for the time moments $T = 0.005$ (a), $T = T_{cl} = 0.15977$ (b), $T = T_M^o = 0.28104$ (c), $T = T_{fr} = 0.42311$ (d), and $T = 0.434$ (e). The areas of islands are colored.

($\mathcal{T} < 0$) by the law

$$X_f^m = |\mathcal{T}|/\sqrt{2(d-1)}, \quad \varrho_f^m = |\mathcal{T}|/\sqrt{2}$$

keeping $\mathcal{T} \leftrightarrow -\mathcal{T}$ symmetry with a sudden reversal of the velocity sign at the contact point of vertices of hyperbola (hyperboloid), $\mathcal{T} = 0$, where, according to Eq. (44), branches of hyperbola (hyperboloid) degenerate in coaxial angles (cones) with $\theta(\Lambda_*) = \tan^{-1} \sqrt{d-1}$ which determine the asymptotes of the hyperbola (hyperboloid) $(|\varrho_f|/X_f)_a = \sqrt{d-1}$.

3. Evolution of islands in the vicinity of coalescence and fragmentation points $\Lambda > \Lambda_*$

Assuming $|\mathcal{T}| \ll \min[(\chi_s - 1)^2, |\chi_M - 1|, T_0]$ where $\chi_M = \chi_s/d = T_M/T_0$, from Eq. (36) we find that evolution of island shape in the vicinity of coalescence and fragmentation points is described by the expression

$$\left(\frac{X_f}{X_f^m}\right)^2 - \left(\frac{\varrho_f}{\varrho_f^m}\right)^2 = \text{sgn}[(\chi_M - 1)\mathcal{T}], \quad (46)$$

where with an increase in T the semiaxes of the hyperbola (hyperboloid of revolution) first contract ($\mathcal{T} > 0$), and then grow ($\mathcal{T} < 0$) by the laws

$$X_f^m = \sqrt{\frac{d|(\chi_M - 1)\mathcal{T}|}{\chi_s(\chi_s - 1)}}$$

and

$$\varrho_f^m = \sqrt{d|(\chi_M - 1)\mathcal{T}|/\chi_s}$$

with the time-independent asymptotes

$$(|\varrho_f|/X_f)_a = \sqrt{\chi_s - 1}.$$

According to Eq. (46), in the coalescence domain ($\chi_M > 1$) vertices of the hyperbola (two-sheet or elliptic hyperboloid) $|X_f^-|$ move toward each other ($\mathcal{T} > 0$), accelerating, up to the coalescence point $\mathcal{T} = 0$, where the semiaxis X_f^m becomes imaginary and ϱ_f^m ($\mathcal{T} < 0$) determines a decelerating increase in width (radius) of the isthmus of the formed two-centered island (one-sheet or hyperbolic hyperboloid). In the fragmentation domain ($1/d < \chi_M < 1$), where the two-centered island divides into two separated islands, this process occurs in a reverse order: hyperbolic hyperboloid ($\mathcal{T} > 0$) \rightarrow elliptic hyperboloid ($\mathcal{T} < 0$). It is remarkable that in the limit of a quasi-1D string $\chi_s - 1 \ll 1$, Eq. (35) allows describing explicitly a complete picture of fragmentation up to the point of individual collapse of each of the islands. For $d > 1$ at $|\mathcal{T}|, |X| \ll 1$ from Eq. (36) we have

$$\mathcal{T}(d-1) = -X_f^2(\chi_s - 1 + \mathcal{T}) + X_f^4/6 + \varrho_f^2 + \dots, \quad (47)$$

from which for the trajectories $X_f^\pm(\mathcal{T})$ of the front points along the X axis ($\varrho_f = 0$) we find

$$(X_f^\pm)^2 = 3(\chi_s - 1 + \mathcal{T}) \pm \sqrt{9(\chi_s - 1 + \mathcal{T})^2 + 6\mathcal{T}(d-1)}$$

and, as a consequence, from the condition $X_f^+(\mathcal{T}_c) = X_f^-(\mathcal{T}_c) = X_c$ for the point of the individual collapse we

get

$$\begin{aligned}\mathcal{T}_c &= -\beta_d(\chi_s - 1)^2[1 - \mathcal{O}(\chi_s - 1) + \dots], \\ X_c &= \sqrt{3(\chi_s - 1 + \mathcal{T}_c)},\end{aligned}$$

where $\beta_d = 3/2(d - 1)$.

Determining further the distance of \pm fronts to the collapse point $\Delta_{\pm} = X_f^{\pm} - X_c$ and assuming that $|\Delta_{\pm}|/X_c \ll 1$ we find from Eq. (47)

$$\Delta_{\pm} = \pm \frac{\sqrt{6(d-1)(\mathcal{T} - \mathcal{T}_c)}}{2X_c} (1 - \Delta_{\pm}/2X_c + \dots),$$

from which it follows that

$$\Delta_+ / |\Delta_-| = 1 - |\Delta_{\pm}|/X_c + \dots \rightarrow 1$$

as $|\Delta_{\pm}|/X_c \propto \sqrt{\mathcal{T} - \mathcal{T}_c}/X_c^2 \rightarrow 0$. Introducing now the difference coordinate $\Delta = X - X_c$, from Eq. (47) we obtain expansion in powers of Δ_f in the form $(d - 1)(\mathcal{T} - \mathcal{T}_c) = -2(\mathcal{T} - \mathcal{T}_c)\Delta_f X_c + (2/3)\Delta_f^2 X_c^2 + \mathcal{O}(X_c \Delta_f^3, \Delta_f^4) + \varrho_f^2 + \dots$, from which it follows that at the final stage of individual collapse $|\Delta_f|/X_c \ll 1$ each of the islands takes the shape of an ellipse (2D) or ellipsoid of revolution (3D) with the center at the collapse point X_c ,

$$\left(\frac{\Delta_f}{\Delta_f^m}\right)^2 + \left(\frac{\varrho_f}{\varrho_f^m}\right)^2 = 1, \quad (48)$$

the semiaxes of which contract by the laws

$$\begin{aligned}\Delta_f^m &= \frac{\sqrt{6(d-1)(\mathcal{T} - \mathcal{T}_c)}}{2X_c}, \\ \varrho_f^m &= \sqrt{(\mathcal{T} - \mathcal{T}_c)(d-1)},\end{aligned}$$

and, consequently, the ellipse (ellipsoid) contracts *self-similarly* up to the collapse point with the *time-independent* aspect ratio

$$\mathcal{A} = \varrho_f^m / \Delta_f^m = \sqrt{2/3} X_c \propto \sqrt{\chi_s - 1},$$

so that $\mathcal{A} \rightarrow 0$ as $\chi_s \rightarrow 1$. According to Eq. (47), during evolution from the fragmentation point $\mathcal{T} = 0$ to the collapse point $\mathcal{T} = \mathcal{T}_c$, the island center almost does not shift $[X_*(0) - X_c]/X_c \propto \chi_s - 1 \ll 1$, the concentration of A particles in the island center decreases by the law $s_c \propto (\mathcal{T} - \mathcal{T}_c)$, and the fraction of particles remaining in the island decreases by the law $\mathcal{N}/\mathcal{N}_0 \propto (\mathcal{T} - \mathcal{T}_c)^{(d+2)/2} / \sqrt{\chi_s - 1}$. As an illustration, Fig. 8 shows the evolution of the shape of 2D islands from the “hyperbolic” ($|\mathcal{T}| \ll |\mathcal{T}_c|$) to the “elliptical” stage ($\mathcal{T} - \mathcal{T}_c \ll |\mathcal{T}_c|$) for $\chi_s - 1 = 0.01$. Below, we shall demonstrate that, as well as in the case of death of the single-centered island ($T_c > T_s$), at the final stage of individual death ($T_c < T_s$) each of the islands takes the shape of an ellipse (ellipsoid of revolution) at any $\Lambda < \Lambda_s$, degenerating into a d -dimensional sphere in the limit of autonomous collapse $\Lambda^{2/d} \ll 1$.

C. Final stage of the individual collapse of islands ($\Lambda < \Lambda_s$)

Let now, as before, $\Delta = X - X_c$, but $\mathcal{T} = (T_c - T)/T_c$ where T_c is the time moment of the individual island collapse ($\Lambda < \Lambda_s$). Then, in the limit of small $\Delta^2/T_c \ll 1$, $\varrho^2/T_c \ll 1$,

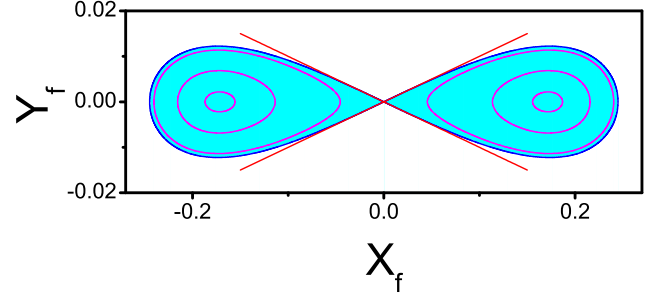


FIG. 8. Evolution of 2D island from the fragmentation ($\mathcal{T} = (T_{fr} - T)/T_{fr} = 0$) to the collapse ($\mathcal{T} = \mathcal{T}_c$) points calculated from Eq. (47) in the quasi-1D string limit $\chi_s - 1 = 0.01$ for the time moments $\mathcal{T} = 0, -2 \times 10^{-5}, -10^{-4}$, and -1.41×10^{-4} .

and $\mathcal{T} \ll 1$ from Eq. (20) we obtain expansion in powers of Δ , ϱ , and \mathcal{T} in the form

$$\frac{s - s_c}{1 + s_c} = \mathcal{F}(\Delta) + \mathcal{E}(\varrho)[1 + \mathcal{F}(\Delta)], \quad (49)$$

where concentration of A particles at the collapse point $\Delta, \varrho = 0$ decreases by the law

$$\begin{aligned}s_c &= \mathcal{T}(d - \chi_c)/2 + m_c \mathcal{T}^2 + \dots, \\ m_c &= \frac{(d+2)}{8}(d - 2\chi_c) + \frac{\chi_c(1 + 3X_c^2)}{16T_c},\end{aligned}$$

and expansions of the functions $\mathcal{F}(\Delta)$ and $\mathcal{E}(\varrho)$ in powers of Δ and ϱ , respectively, have the form

$$\mathcal{F}(\Delta) = c_1 \Delta + c_2 \Delta^2 + c_3 \Delta^3 + c_4 \Delta^4 + \dots$$

and

$$\mathcal{E}(\varrho) = -\varrho^2(1 + \mathcal{T} - \varrho^2/8T_c + \dots)/4T_c + \dots,$$

where the coefficients

$$\begin{aligned}c_1 &= \frac{\chi_c X_c \mathcal{T}}{2T_c} [1 + \mathcal{O}(\mathcal{T}) + \dots], \\ c_2 &= -\frac{1 - \chi_c + \omega \mathcal{T} + \dots}{4T_c}, \\ \omega &= 1 + \chi_c (X_c^2/T_c - 2), \\ c_3 &= -\frac{\chi_c X_c}{12T_c^2} [1 + \mathcal{O}(\mathcal{T}) + \dots], \\ c_4 &= \frac{1 + \chi_c (X_c^2/2T_c + 1/6T_c - 2)}{32T_c^2} [1 + \mathcal{O}(\mathcal{T}) + \dots],\end{aligned}$$

and the notation is introduced

$$0 < \chi_c = \frac{(1 - X_c^2)}{2T_c} < 1. \quad (50)$$

From Eq. (49) we conclude that at any $\Lambda < \Lambda_s$ at the final collapse stage $\mathcal{T} \rightarrow 0$ the distribution of particles in each of the islands takes the universal scaling form

$$s = \mathcal{T} \mathcal{S}_{d,\Lambda} \left(\frac{|\Delta|}{\mathcal{T}^{1/2}}, \frac{|\varrho|}{\mathcal{T}^{1/2}} \right), \quad (51)$$

from which, according to Eq. (49), it follows that in 1D systems in the domain $X \geq 0$ the fronts $\Delta_{\pm} = X_f^{\pm} - X_c$

asymptotically converge symmetrically to the collapse point $\Delta_{\pm} = 0$ by the law

$$\Delta_{\pm} = \pm \Delta_f^m = \pm \sqrt{2T_c \mathcal{T}}.$$

Correspondingly, in agreement with Eq. (48), in 2D and 3D systems each of the islands takes asymptotically the shape of an ellipse (2D) or ellipsoid of revolution (3D) the semiaxes of which contract by the laws

$$\Delta_f^m = \sqrt{\frac{2T_c(d - \chi_c)\mathcal{T}}{(1 - \chi_c)}}, \quad (52)$$

$$\varrho_f^m = \sqrt{2T_c(d - \chi_c)\mathcal{T}}, \quad (53)$$

and, consequently, the ellipse (ellipsoid) contracts *self-similarly* up to the collapse point with the time-independent aspect ratio

$$\mathcal{A} = \varrho_f^m / \Delta_f^m = \sqrt{1 - \chi_c}.$$

According to Eq. (22), in the limit $\Lambda \rightarrow \Lambda_s$ we find from Eq. (50) $1 - \chi_c = 2X_c^2/3 + \dots \rightarrow 0$ as $T_c \rightarrow T_s$, whereas in the opposite limit $\Lambda/\Lambda_s \ll 1$ ($T_c \ll T_s$) the value of χ_c rapidly becomes exponentially small with a decrease in Λ : $\chi_c \propto e^{-1/2T_c}/T_c \rightarrow 0$ as $T_c \rightarrow 0$. Thus, we conclude that in the limit $\Lambda \rightarrow \Lambda_s$ ($\chi_c \rightarrow 1$), as expected, the island ‘‘inherits’’ the shape of a quasi-1D string $\mathcal{A}(\chi_c \rightarrow 1) \rightarrow 0$, whereas, in agreement with Eq. (28), in the opposite limit of autonomous death $\Lambda \ll \Lambda_s$ ($\chi_c \ll 1$) the island contracts self-similarly in the form of a d -dimensional sphere $\mathcal{A}(\chi_c \rightarrow 0) \rightarrow 1$.

In the general case for the trajectories of crossover to the regime of self-similar collapse of \pm fronts along the $X(\varrho_f = 0)$ axis, we obtain from Eq. (49)

$$\Delta_{\pm} = \pm \Delta_f^m (1 \mp q\mathcal{T}^{1/2} + g\mathcal{T} + \dots), \quad (54)$$

where

$$q = \frac{\chi_c X_c \sqrt{2(d - \chi_c)/T_c}}{6(1 - \chi_c)^{3/2}} (1 - \Gamma), \quad \Gamma = \frac{3(1 - \chi_c)}{(d - \chi_c)}$$

and

$$g = \frac{m_c}{d - \chi_c} - \frac{\omega}{2(1 - \chi_c)} + (d - \chi_c) \left[\frac{c_4 T_c}{|c_2|(1 - \chi_c)} - 1/4 \right].$$

Determining the domain of self-similar island collapse by the condition $\text{Max}|\Delta_{\pm}|/\Delta_f^m - 1| < \epsilon \ll 1$ we find from Eq. (54) that in the limit of small $1 - \chi_c \ll 1$, the boundary of this domain is determined by the dominant term $q\mathcal{T}^{1/2}$,

$$\mathcal{T}_{\pm} \sim (\epsilon/q)^2 \sim \frac{6(1 - \chi_c)^2 \epsilon^2}{(d - \chi_c)(1 - \Gamma)^2}, \quad (55)$$

whereas in the opposite limit $\chi_c \sim \exp(-1/2T_c)/T_c \ll 1$ the boundary of this domain [in agreement with the dynamics of autonomous collapse of the d -dimensional sphere, Eq. (28)] is determined by the dominant term $g\mathcal{T}$,

$$\mathcal{T}_{\pm} \sim \epsilon/|g| \sim 4\epsilon. \quad (56)$$

In Fig. 9 are shown the dependencies $\mathcal{T}_{+}(T_c)$ and $\mathcal{T}_{-}(T_c)$ for $\epsilon = 0.01$ which demonstrate the key features of crossover to the regime of self-similar collapse of \pm fronts at $d = 1, 2$, and 3. It is seen that in 1D and 3D systems the boundary of the self-similar collapse regime $\text{Max}|\Delta_{\pm}|/\Delta_f^m - 1| = \epsilon$ is

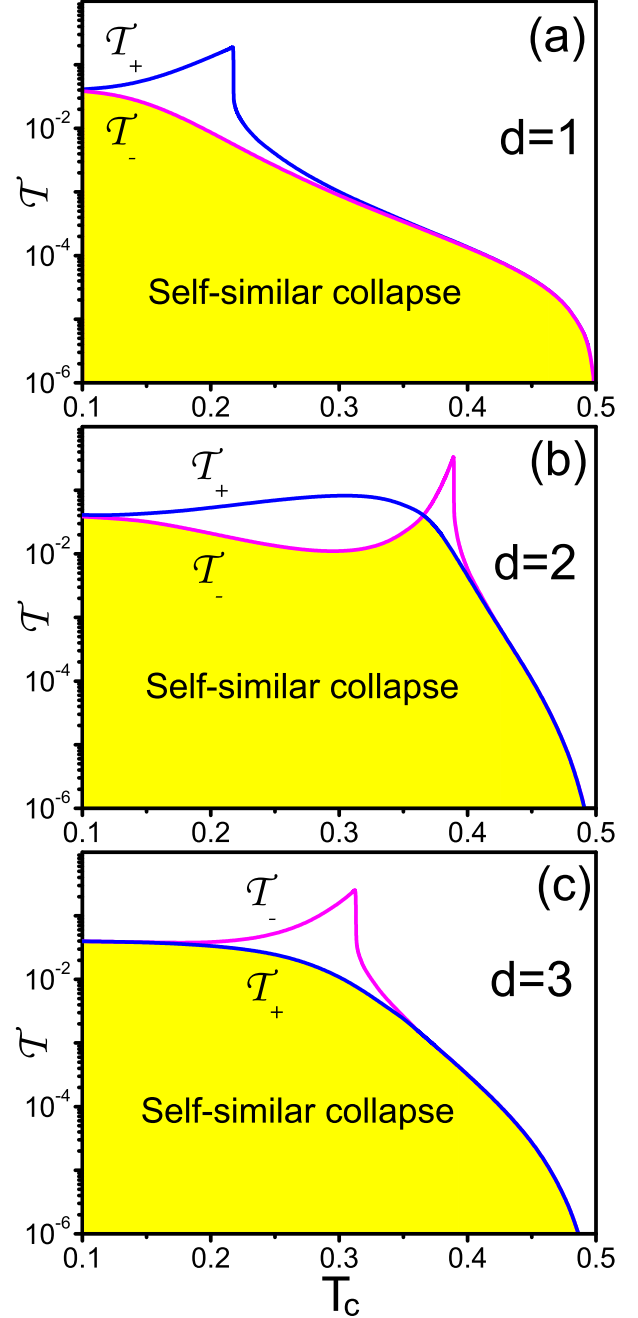


FIG. 9. Dependencies $\mathcal{T}_{\pm}(T_c)$ calculated from Eq. (21) at $\epsilon = 0.01$ for 1D (a), 2D (b), and 3D (c) systems. The areas of self-similar collapse are colored.

determined by evolution of either the front Δ_{-} ($d = 1, q < 0$) or the front Δ_{+} ($d = 3, q > 0$), whereas in the 2D case this boundary is determined by evolution of the front Δ_{-} in the range $0 < \chi_c < 1/2$ ($q < 0$) and by evolution of the front Δ_{+} in the range $1/2 < \chi_c < 1$ ($q > 0$). We emphasize that according to Eqs. (55) and (56) in the ranges $T_c < 0.1$ and $T_c > 0.3-0.4$, both of the fronts reach the boundary of the self-similar collapse regime simultaneously. Moreover, the detailed analysis shows that in 1D systems $\Delta_{+} > |\Delta_{-}|$, in 3D systems $\Delta_{+} < |\Delta_{-}|$, and in 2D systems $\Delta_{+} > |\Delta_{-}|$ in the range $0 < \chi_c < 1/2$, whereas in the range $1/2 < \chi_c < 1$,

where the individual collapse is preceded by coalescence fragmentation $\Delta_+ < |\Delta_-|$. According to Eq. (49), in 2D and 3D systems the ‘‘trajectory’’ of crossover to the regime of self-similar contraction of minor semiaxis of the ellipse (ellipsoid) has the form

$$|\varrho_f(\Delta = 0)| = \varrho_f^m(1 + \phi\mathcal{T} + \dots),$$

where $\phi = m_c/(d - \chi_c) - (d - \chi_c)/8 - 1/2$, from which it follows that in fulfilling the requirement $\text{Max}|\Delta_{\pm}|/\Delta_f^m - 1| < \epsilon$, the condition $|\varrho_f(\Delta = 0)|/\varrho_f^m - 1| < \epsilon$ is satisfied automatically in the entire range $0 < \Lambda < \Lambda_s$.

It is easy to see that, as it should be, in the collapse area of a single-centered island, $\Lambda > \Lambda_s$, Eq. (54) is transformed into Eq. (41), where $X_c = 0$, $\chi = \chi_c = 1/2T_c$, $q = 0$, $\mu = g$, $X_f^m = \Delta_f^m$, and $\mathcal{T}(\epsilon) \sim \epsilon/|\mu|$ in the whole range $T_c > T_s$.

VI. EVOLUTION, DELOCALIZATION, AND RELOCALIZATION OF THE REACTION FRONT

So far we have assumed that the reaction front is sharp enough so that the front relative width remains negligibly small and, as a consequence, the front moves quasistatically up to a narrow vicinity of the island collapse point. In this section, we shall reveal the conditions for this assumption realization.

In Refs. [17,18,22,23] it has been established that at $d > d_c = 2$ in the dimensional variables the dependence of the quasistatic front width w on the boundary current density J is described by the mean-field law

$$w_{\text{MF}} \sim (D^2/kJ)^{1/3}, \quad (57)$$

whereas in the 1D case in the diffusion-controlled limit the quasistatic front width becomes k independent and it is determined by the fluctuation law

$$w_{\text{F}} \sim \sqrt{D/J}$$

[at upper critical dimension $d_c = 2$ in the mean-field law (57) a logarithmic correction appears [20,37]].

As noted in the Introduction, in the case of autonomous evolution of the d -dimensional spherical island, an exhaustive analysis of the reaction front relative width evolution for the fluctuation, the logarithmically modified, and the mean-field regimes was presented [37]. It was demonstrated that in a wide range of parameters at a large enough initial island particle number the front remains sharp up to a narrow vicinity of the island collapse point and, therefore, the whole picture of island evolution is completely self-consistent. According to Ref. [37] in the mean-field regime (i.e., for quasi-1D, quasi-2D, and 3D systems) regardless of the system dimension and the initial number of island particles, evolution of the relative front width $\eta = w/r_f$ is described by a universal law within which the characteristic time of front delocalization at the final collapse stage is determined unambiguously by the relative width of the front at its turning point $\mathcal{T}_Q \sim \eta_M^{3/2}$.

From the analysis presented above, it is clear that in the problem of evolution of the island-sea-island system behavior of the front width becomes much more complicated except for the limits of small and large Λ , where the majority of particles die in the regime of evolution of the d -dimensional sphere. Fortunately, the detailed description of behavior of the

front width $w(\mathbf{r}_f, \Lambda, T)$ is not necessary. Indeed, just as in the case of evolution of the d -dimensional sphere, we will be primarily interested in revealing the parameter domain within which the front delocalization occurs at the final (self-similar) collapse stage where the front width grows unlimitedly as T approaches the collapse point T_c . Our second main aim will be to determine the parameter domain within which front delocalization occurs in a narrow vicinity of the points of coalescence T_{cl} and fragmentation T_{fr} where the front width increases unlimitedly as the front approaches the system center.

To avoid unnecessary complications, we will consider evolution of the front in the mean-field regime for quasi-1D, quasi-2D, and 3D systems. According to Eq. (57), in the units that we have accepted, the mean-field front width reads as

$$w \sim 1/(\kappa J)^{1/3}, \quad (58)$$

where the effective reaction constant $\kappa = kb_0\ell^2/D$ and the boundary current density $J = |\nabla s|_{|\mathbf{r}_f} = [\sqrt{(\partial_X s)^2 + (\partial_\rho s)^2}]_{|\mathbf{r}_f}$.

A. Final stage of the individual collapse of islands ($\Lambda < \Lambda_s$)

At $\Lambda < \Lambda_s$ from Eq. (49) we find that on the final (self-similar) collapse stage the relative width of the reaction front along the X axis increases by the law

$$\eta_\Delta^m = w_\Delta/\Delta_f^m = \left(\frac{\mathcal{T}_\Delta^Q}{\mathcal{T}}\right)^{2/3}, \quad (59)$$

where the characteristic time of front delocalization is

$$\mathcal{T}_\Delta^Q = \sqrt{\frac{(1 - \chi_c)}{2\kappa T_c(d - \chi_c)^2}}. \quad (60)$$

In the quasi-2D and 3D systems, Eqs. (59) and (60) determine the evolution of the relative front width along the major semiaxis of the ellipse (ellipsoid), whereas the evolution of the relative front width along the minor semiaxis of the ellipse (ellipsoid) is determined by the law

$$\eta_\varrho^m = w_\varrho/\varrho_f^m = \left(\frac{\mathcal{T}_\varrho^Q}{\mathcal{T}}\right)^{2/3}, \quad (61)$$

where the characteristic time of front delocalization is

$$\mathcal{T}_\varrho^Q = 1/\sqrt{2\kappa T_c(d - \chi_c)^2}. \quad (62)$$

According to Eqs. (60) and (62), $\mathcal{T}_\Delta^Q/\mathcal{T}_\varrho^Q = \sqrt{1 - \chi_c} < 1$, hence, since the front width varies monotonically along its $\Delta_m \rightarrow \varrho_m$ contour, \mathcal{T}_Δ^Q and \mathcal{T}_ϱ^Q determine, respectively, the low and upper bounds of the characteristic time of front delocalization.

In the limit of autonomous collapse of the d -dimensional sphere $\chi_c \ll 1$ ($T_c \ll T_s$) at $\sqrt{\kappa T_c} \gg 1$ we find

$$\mathcal{T}_\Delta^Q \approx \mathcal{T}_\varrho^Q = 1/d(2\kappa T_c)^{1/2} \quad (63)$$

from which, in combination with Eqs. (52) and (53), for the characteristic radius of front delocalization it follows

$$\Delta_f^Q \approx \varrho_f^Q = \left(\frac{2T_c}{\kappa}\right)^{1/4}. \quad (64)$$

In the opposite limit $1 - \chi_c \ll 1$ [i.e., in the vicinity of the threshold of single-centered island collapse $(T_s - T_c)/T_s \ll 1$] we have $\mathcal{T}_\Delta^Q \ll \mathcal{T}_\rho^Q$ and, consequently, in a drastic contrast to the quasi-1D case, at $d > 1$ the front delocalization occurs along the minor semiaxis of the ellipse (ellipsoid), that is why these systems should be considered separately.

1. Quasi-1D systems

Satisfying the condition of self-similar collapse $\mathcal{T}_\rho^\Delta \ll 1 - \chi_c \ll 1$ we find from Eq. (60) that this condition is complied at

$$1 - \chi_c \gg \kappa^{-1/3}$$

from which, according to Eqs. (52) and (60), we derive

$$\begin{aligned} \kappa^{-1/2} &\ll \mathcal{T}_\Delta^Q \sim \frac{1}{\sqrt{\kappa(1 - \chi_c)}} \ll \kappa^{-1/3}, \\ \kappa^{-1/4} &\ll \Delta_m^Q \sim \frac{1}{[\kappa(1 - \chi_c)]^{1/4}} \ll \kappa^{-1/6}. \end{aligned} \quad (65)$$

In the opposite limit $1 - \chi_c \ll \mathcal{T}_X^Q \ll 1$, long before reaching the regime of self-similar collapse (51), front delocalization occurs in the self-similar regime (38) from which it follows that

$$\eta_X = w_X/X_f = \mathcal{T}_X^Q/\mathcal{T}, \quad (66)$$

where

$$\mathcal{T}_X^Q \sim \kappa^{-1/3}, \quad X_f^Q \sim \kappa^{-1/6}. \quad (67)$$

2. Quasi-2D and 3D systems

According to Eqs. (60) and (62), at $d > 1$ in the vicinity of the threshold of single-centered island collapse $1 - \chi_c \ll 1$, the characteristic time of front delocalization is determined by the value $\mathcal{T}_\rho^Q \gg \mathcal{T}_\Delta^Q$, that is why the condition for crossover to the self-similar collapse regime (51) is the requirement $\mathcal{T}_\rho^Q \ll (1 - \chi_c)^2$ from which it follows

$$1 - \chi_c \gg \kappa^{-1/4}$$

and so we have

$$\begin{aligned} \mathcal{T}_\rho^Q &\sim 1/[\kappa(d - \chi_c)^2]^{1/2} \sim \kappa^{-1/2}, \\ \kappa^{-1/4} &\ll \Delta_m^Q \ll \kappa^{-1/8}, \quad \rho_m^Q \sim \kappa^{-1/4} \end{aligned} \quad (68)$$

with the aspect ratio

$$\kappa^{-1/8} \ll \mathcal{A}_Q \ll 1.$$

In the opposite limit $1 - \chi_c \ll \kappa^{-1/4}$, long before reaching the regime of self-similar collapse, front delocalization occurs at the stage of superellipse (superellipsoid) evolution $1 - \chi_c \ll \mathcal{T} \ll 1$ where, according to Eq. (40), the relative front width along the major semiaxis of superellipse grows by the law

$$\eta_X = w_X/X_f^m = \left(\frac{\mathcal{T}_X^Q}{\mathcal{T}} \right)^{1/2}, \quad (69)$$

where $X_f^m = [6\mathcal{T}(d - \chi_c)]^{1/4}$ and $\mathcal{T}_X^Q \sim \kappa^{-2/3}$. According to Eq. (61), as well as in the case of Δ collapse, the relative front width of superellipse (superellipsoid) along its minor semiaxis grows by the law (61) and determines the characteristic time

of front delocalization $\mathcal{T}_\rho^Q \sim 1/\kappa^{1/2}(d - \chi_c) > \mathcal{T}_X^Q$. Assuming further that $1 - \chi_c \sim X_c^2 \ll \mathcal{T}_\rho^Q \sim \kappa^{-1/2}$ (including the critical point $X_c = 0, \Lambda = \Lambda_s$), we find

$$X_f^Q \sim \kappa^{-1/8}, \quad \rho_f^Q \sim \kappa^{-1/4} \quad (70)$$

with the aspect ratio

$$\mathcal{A}_Q \sim \kappa^{-1/8}$$

so that $\mathcal{A} \rightarrow 0$ as $\kappa \rightarrow \infty$ [note that as it should be $X_c \ll (X_f^Q)^2 \ll X_f^Q \ll 1$].

B. Final stage of collapse of the single-centered island ($\Lambda > \Lambda_s$)

According to Eq. (41) at $\Lambda > \Lambda_s \geq \Lambda_*$ the island coalescence is completed by the self-similar collapse of single-centered island in the system center $X_c = 0$. Repeating the calculations of the previous section, it is not difficult to demonstrate that all the results obtained above for the individual collapse of islands remain valid for the collapse of the single-centered island, with the only difference being that at $\Lambda > \Lambda_s \Delta_f^m = X_f^m$ and $\chi_c = \chi = 1/2T_c$.

C. Evolution of the reaction front in the vicinity of coalescence point T_{cl}

In a drastic contrast to autonomous evolution of the d -dimensional spherical island, where front delocalization occurs only at the final collapse stage, at $\Lambda > \Lambda_*$ the relative front width along the X axis starts increasing unlimitedly as the leading point of the front X_f^- approaches the system center (where $J \rightarrow 0$ and hence $w_X \rightarrow \infty$ as $T \rightarrow T_{cl}$) and, as a consequence, the *intermediate* front delocalization arises.

Assuming that $|\mathcal{T}| = |T_{cl} - T|/T_{cl} \ll \min[(\chi_M - 1), T_{cl}]$ we find from Eq. (35)

$$\eta_X^m = w_X/X_f^m = (\mathcal{T}_X^Q/\mathcal{T})^{2/3}, \quad (71)$$

where the characteristic time of front delocalization is

$$\mathcal{T}_X^Q = \sqrt{\frac{(\chi_s - 1)}{2\kappa T_{cl}(\chi_s - d)^2}} \quad (72)$$

from which, according to Eq. (46), the characteristic ‘‘length’’ of delocalization is

$$X_f^Q \sim \left(\frac{2T_{cl}}{\kappa(\chi_s - 1)} \right)^{1/4}. \quad (73)$$

Far from the critical point $\Lambda \gg \Lambda_*$ ($\chi_M = \chi_s/d = 1/2dT_{cl} \gg 1$) from Eqs. (72) and (73) at any d it follows

$$\mathcal{T}_X^Q \sim \kappa^{-1/2}, \quad X_f^Q \sim (T_{cl}^2/\kappa)^{1/4} \quad (74)$$

from which satisfying condition $\mathcal{T}_X^Q \ll T_{cl} \ll 1$ we conclude

$$T_{cl} \gg \kappa^{-1/2}, \quad \kappa^{-1/2} \ll X_f^Q \ll \kappa^{-1/4}.$$

In the vicinity of the critical point $\Lambda \sim \Lambda_*$, behavior of the relative front width at $d = 1$ and $d > 1$ differs qualitatively.

1. Quasi-1D systems

Assuming that $\chi_M - 1 = \chi_s - 1 \ll 1$ and satisfying the condition of self-similar coalescence regime $\mathcal{T}_X^Q \ll \chi_M - 1$,

from Eq. (72) we find that this requirement is fulfilled at

$$\chi_s - 1 \gg \kappa^{-1/3}$$

from which, according to Eqs. (72) and (73), it follows

$$\kappa^{-1/2} \ll \mathcal{T}_X^Q \ll \kappa^{-1/3}, \quad \kappa^{-1/4} \ll X_f^Q \ll \kappa^{-1/6}.$$

In the opposite limit $\chi_M - 1 \ll \mathcal{T}_X^Q \ll 1$, long before reaching the self-similar coalescence regime (46) front delocalization occurs in the self-similar regime (38) from which, as well as in the case of collapse, Eqs. (66) and (67) follow.

2. Quasi-2D and 3D systems at $T < T_{cl}$

Satisfying the condition of the self-similar coalescence regime $\mathcal{T}_X^Q \ll \chi_M - 1 \ll 1$ in the vicinity of the critical point $\chi_M - 1 \ll 1$, from Eq. (72) we find that this requirement is fulfilled at

$$\chi_M - 1 \gg \kappa^{-1/4}$$

from which, according to Eqs. (72) and (73), it follows

$$\kappa^{-1/2} \ll \mathcal{T}_X^Q \ll \kappa^{-1/4}, \quad X_f^Q \sim \kappa^{-1/4}.$$

In the opposite limit $\chi_M - 1 \ll \mathcal{T}_X^Q \ll 1$ (including the critical point $\chi_M = 1$), according to Eq. (45), the front moves with a constant velocity and we derive

$$\eta_X^m = w_X/X_f^m = \left(\frac{\mathcal{T}_X^Q}{\mathcal{T}} \right)^{4/3}, \quad (75)$$

where the characteristic time of front delocalization is

$$\mathcal{T}_X^Q = \sqrt{2} \left(\frac{d-1}{\kappa d} \right)^{1/4} \sim \kappa^{-1/4} \quad (76)$$

and, hence, the characteristic length of delocalization is

$$X_f^Q = [d(d-1)\kappa]^{-1/4} \sim \kappa^{-1/4}. \quad (77)$$

3. Quasi-2D and 3D systems at $T > T_{cl}$

According to Eq. (35), at $\mathcal{T} < 0$ in the system center $\mathbf{r} = 0$ an excess of A particles arises with an increase in which an isthmus between the islands is formed limited by the sharp reaction front. From Eqs. (35) and (46) it follows that under the condition $|\mathcal{T}| \ll T_{cl}$ with growing $|\mathcal{T}|$ the relative front width in the plane $X = 0$, where radius of the isthmus is minimal, contracts by the law

$$\eta_\varrho = w_\varrho/\varrho_f^m = (\mathcal{T}_\varrho^Q/|\mathcal{T}|)^{2/3}, \quad (78)$$

where the characteristic time of formation of a two-centered island limited by the sharp front is

$$\mathcal{T}_\varrho^Q = \sqrt{\frac{\chi_s}{\kappa(\chi_s - d)^2}} \quad (79)$$

and the corresponding characteristic radius of the isthmus is

$$\varrho_f^Q = (2T_{cl}/\kappa)^{1/4}. \quad (80)$$

In the limit of large $\chi_M \gg 1$ ($T_{cl} \ll T_M$) from Eq. (79) we obtain $\mathcal{T}_\varrho^Q = \sqrt{2T_{cl}/\kappa}$ from which satisfying the requirement $\mathcal{T}_\varrho^Q \ll T_{cl}$ we find $\kappa^{-1} \ll T_{cl} \ll T_M$ and, therefore, we conclude

$$\kappa^{-1} \ll \mathcal{T}_\varrho^Q \ll \kappa^{-1/2}, \quad \kappa^{-1/2} \ll \varrho_f^Q \ll \kappa^{-1/4}. \quad (81)$$

In the opposite limit $\chi_M - 1 \ll 1$, by satisfying the condition of the self-similar coalescence regime $\mathcal{T}_\varrho^Q \ll \chi_M - 1$ from Eq. (79) we find $\chi_M - 1 \gg \kappa^{-1/4}$ from which it follows that

$$\kappa^{-1/2} \ll \mathcal{T}_\varrho^Q \ll \kappa^{-1/4}, \quad \varrho_f^Q \sim \kappa^{-1/4}. \quad (82)$$

According to Eq. (35), at $\chi_M - 1 \ll |\mathcal{T}| \ll 1$ in the system center $\mathbf{r} = 0$ an excess of sea particles arises and, consequently, in the vicinity of coalescence threshold $\chi_M - 1 \ll \kappa^{-1/4}$ no isthmus between the islands is formed. We conclude thus that formation of a two-centered dumbbell-like island limited by the sharp front occurs only in the domain $\chi_M - 1 \gg \kappa^{-1/4}$.

D. Evolution of the reaction front in the vicinity of fragmentation point T_{fr}

1. Quasi-2D and 3D systems at $T < T_{fr}$

According to Eq. (35), in the domain $\mathcal{T} = (T_{fr} - T)/T_{fr} \ll 1 - \chi_M$, as the excess of A particles in the system center decreases, the half-width (radius) of the isthmus in the $X = 0$ plane contracts by the law (46), from which it follows that with growing T the relative front width increases by the law (78) where the characteristic time of front delocalization and the corresponding characteristic half-width (radius) of the isthmus are determined by Eqs. (78) and (80) with $T_{fr}(1 < \chi_s = T_s/T_{fr} < d)$ instead of $T_{cl}(d < \chi_s = T_s/T_{cl} < \infty)$. As expected, in the vicinity of fragmentation threshold $1 - \chi_M \ll 1$ the front delocalization occurs only in the domain $1 - \chi_M \gg \kappa^{-1/4}$ where at the coalescence stage the front localization occurs:

$$(w \downarrow)\varrho_f \leftarrow \mathbf{0} \rightarrow -\varrho_f(w \downarrow), |\mathcal{T}| \uparrow, \quad (cl, loc)$$

$$(w \uparrow)\varrho_f \rightarrow \mathbf{0} \leftarrow -\varrho_f(w \uparrow), \mathcal{T} \downarrow, \quad (fr, deloc).$$

Not too close to the fragmentation threshold up to the threshold of single-centered island $\chi_s \sim 1$ we find from Eqs. (79) and (80)

$$\mathcal{T}_\varrho^Q \sim \kappa^{-1/2}, \quad \varrho_f^Q \sim \kappa^{-1/4}. \quad (83)$$

2. Quasi-2D and 3D systems at $T > T_{fr}$

Just as during coalescence the front delocalization occurs in the vicinity of vertices of the hyperbola (hyperboloid) $|X_f^-|$ moving toward each other,

$$(w \uparrow)X_f^- \rightarrow \mathbf{0} \leftarrow -X_f^-(w \uparrow), \mathcal{T} \downarrow, \quad (cl, deloc)$$

at the final fragmentation stage the formation of the localized front is completed in the vicinity of the vertices $|X_f^-|$ moving away from each other,

$$(w \downarrow)X_f^- \leftarrow \mathbf{0} \rightarrow -X_f^-(w \downarrow), |\mathcal{T}| \uparrow, \quad (fr, loc).$$

According to Eq. (35), at $|\mathcal{T}| \ll \min[(\chi_s - 1)^2, |\chi_M - 1|, T_{fr}]$ with an increase in $|\mathcal{T}|$ the relative front width in the vertices vicinity contracts by the law

$$\eta_X^m = w_X/X_f^m = (\mathcal{T}_X^Q/|\mathcal{T}|)^{2/3}, \quad (84)$$

where the characteristic time of front localization is

$$\mathcal{T}_X^Q = \sqrt{\frac{(\chi_s - 1)}{2\kappa T_{fr}(\chi_s - d)^2}} \quad (85)$$

and the characteristic length of localization is

$$X_f^Q \sim \left(\frac{2T_{fr}}{\kappa(\chi_s - 1)} \right)^{1/4}. \quad (86)$$

According to Eqs. (85) and (86), the characteristic features of the front localization are reduced to the following:

(i) From Eqs. (72) and (85) we conclude that, as expected, in the vicinity of the coalescence-fragmentation threshold $1 - \chi_M \ll 1$ a remarkable symmetry takes place

$$\eta_X(cl, \mathcal{T}) \leftrightarrow \eta_X(fr, -\mathcal{T})$$

and, as a consequence, in the domain $\kappa^{-1/4} \ll 1 - \chi_M \ll 1$ the characteristic time of front localization $\mathcal{T}_X^Q(fr) \ll \kappa^{-1/4}$, whereas in the domain of elastic front reflection $1 - \chi_M \ll \kappa^{-1/4}$ we return to Eqs. (76) and (77).

(ii) Much more nontrivial is the front localization in the limit of a quasi-1D string $\chi_s - 1 \ll 1$. Assuming that $\mathcal{T}_X^Q \ll |\mathcal{T}_c| \sim (\chi_s - 1)^2$ we derive from Eq. (85) that the front localization is completed long before the collapse of the island in the domain $\chi_s - 1 \gg \kappa^{-1/3}$ where $\kappa^{-2/3} \ll \mathcal{T}_X^Q \ll |\mathcal{T}_c|$ and $X_f^Q \ll \kappa^{-1/6} \ll X_c \sim \sqrt{\chi_s - 1}$. It is clear, however, that fragmentation is completed by the formation of separated daughter islands with the sharp front only under the condition that by the moment \mathcal{T}_X^Q of front localization along the X axis the relative front width η_ρ^c along the ρ axis, outgoing from the island center, remains small enough. From Eqs. (35) and (47) we obtain easily that at $\mathcal{T}_X^Q/|\mathcal{T}_c| \ll 1$, fragmentation is completed by the formation of separated islands with the sharp front under fulfilling the more rigid condition $\chi_s - 1 \gg \kappa^{-1/4}$ (note that this condition correlates with the condition of self-similar Δ collapse $1 - \chi_c \gg \kappa^{-1/4}$). We conclude thus that in the vicinity of the critical point $\chi_s - 1 \ll \kappa^{-1/4}$ the fragmentation of the quasi-1D string is completed by loss of individuality (mixing with the sea) of the daughter islands long before occurrence of the self-similar collapse stage.

(iii) In the domain of intermediate $\Lambda_* < \Lambda < \Lambda_s$ not too close to the threshold points Λ_* and Λ_s we find from Eqs. (85) and (86)

$$\mathcal{T}_X^Q \sim \kappa^{-1/2}, \quad X_f^Q \sim \kappa^{-1/4}. \quad (87)$$

The presented analysis of the key features of evolution of the reaction front shows that the revealed picture of island coalescence, fragmentation, and collapse is completely self-consistent only in the limit when the effective reaction constant $\kappa = kb_0\ell^2/D$ is large enough. In the next section, our aim will be to demonstrate that in the diffusion-controlled annihilation regime, the value of κ is large indeed in a wide range of parameters.

VII. EVOLUTION OF THE FRONT IN THE DIFFUSION-CONTROLLED ANNIHILATION REGIME

Extracting the parameter Λ in κ explicitly, we obtain

$$\kappa = \frac{ka_0\ell^2}{cD} = \frac{ka_0\ell^2}{\Lambda DL^d} = \frac{ka_0h^d\ell^{2-d}}{\Lambda D}$$

from which, substituting here the constant of diffusion-controlled annihilation in the 3D medium $k = \zeta Dr_a$ where r_a

is the annihilation radius and $\zeta = 8\pi$, we find

$$\kappa = \mathcal{K}/\Lambda, \quad \mathcal{K} = \zeta r_a a_0 h^d \ell^{2-d}. \quad (88)$$

From Eq. (88) it follows that (i) at fixed values of Λ , a_0 , and $L = \ell/h$ a simultaneous increase in the initial size of the island and the initial distance between the islands results in a rapid growth of $\mathcal{K} \propto \ell^2$; (ii) at fixed values of Λ , a_0 , and h (i.e., at fixed initial particle number in the island) with growing ℓ the value of \mathcal{K} increases in quasi-1D systems, *does not change* in quasi-2D systems, and decreases in 3D systems as a consequence of a decrease in the initial sea density $\propto 1/\ell^d$:

$$\mathcal{K} \sim \begin{cases} \text{const} \ell, & d = 1 \\ \text{const}, & d = 2 \\ \text{const}/\ell, & d = 3. \end{cases}$$

Taking for illustration the realistic values $r_a \sim 10^{-8}$ cm, $a_0 \sim 10^{23}$ cm $^{-3}$, $h = 0.1$ cm, and $\ell = 10$ cm we find from Eq. (88) $\mathcal{K} \sim 10^{16}$ for $d = 1$, $\mathcal{K} \sim 10^{14}$ for $d = 2$, and $\mathcal{K} \sim 10^{12}$ for $d = 3$. Below, we will use these values of \mathcal{K} to estimate the typical domains of front delocalization.

A. Collapse

1. Autonomous and single-centered collapse of spherical islands

According to Eq. (28), in the limit of small $1/L^2 \ll \Lambda^{2/d} \ll 1$ evolution of each of the islands occurs in the autonomous regime in the shape of a d -dimensional sphere with the centers at the points $X_c \sim \pm 1$, whereas in the limit of large $\Lambda^{2/d} \gg 1$ evolution of the formed by coalescence single-centered island occurs in the shape of a d -dimensional sphere with the center at the point $X_c = 0$. It is remarkable that in both limits evolution of the radius of the island $\rho_f(T)$ and particle distribution in it is described by the universal scaling laws (16) and (28) [37] with the Λ -dependent time of island collapse $T_c \sim \Lambda^{2/d}$. Substituting T_c into Eqs. (63) and (64), for the characteristic time \mathcal{T}_Q and radius ρ_f^Q of front delocalization at the final collapse stage we obtain

$$\mathcal{T}_Q \sim (\mathcal{K}\Lambda^{(2-d)/d})^{-1/2}, \quad \rho_f^Q \sim (\Lambda^{(d+2)/d}/\mathcal{K})^{1/4}$$

from which taking into account the accepted parameters it follows

$$\mathcal{T}_Q \sim \begin{cases} 10^{-8}/\Lambda^{1/2}, & d = 1 \\ 10^{-7}, & d = 2 \\ 10^{-6}\Lambda^{1/6}, & d = 3 \end{cases} \quad (89)$$

and

$$\rho_f^Q \sim \begin{cases} 10^{-4}\Lambda^{3/4}, & d = 1 \\ 10^{-7/2}\Lambda^{1/2}, & d = 2 \\ 10^{-3}\Lambda^{5/12}, & d = 3. \end{cases} \quad (90)$$

Since, with the parameters fixed by us, an increase in $\Lambda \propto \text{const}/b_0$ corresponds to a decrease in the initial sea density b_0 , from Eq. (89) it follows that with a decrease in the initial sea density the characteristic time of front delocalization \mathcal{T}_Q decreases at $d = 1$, *does not change* at $d = 2$, and increases slowly at $d = 3$ remaining small in a wide range of Λ . We conclude thus that in a wide range of small and large Λ the front remains sharp up to a narrow vicinity of the collapse point. According to Eq. (90), at any d the characteristic

delocalization radius ρ_f^Q increases with growing Λ , remaining relatively small in a wide range of Λ . More revealing is the ratio $\Xi_Q = \rho_f^Q / \rho_f^M$ of the delocalization radius to the radius of maximal island expansion $\rho_f^M \sim \Lambda^{1/d}$ at the front turning point

$$\Xi_Q \sim \sqrt{\mathcal{T}_Q} \sim \begin{cases} 10^{-4}/\Lambda^{1/4}, & d = 1 \\ 10^{-7/2}, & d = 2 \\ 10^{-3}\Lambda^{1/12}, & d = 3. \end{cases}$$

Here, it should be emphasized a remarkable fact that at $d = 2$ this ratio, as well as \mathcal{T}_Q and the relative front width at the turning point $\eta_\rho^M \sim \mathcal{T}_Q^{2/3}$ [37], does not depend on the initial sea density.

2. Collapse of islands in the vicinity of the critical point $\Lambda \sim \Lambda_*$

In the quasi-1D case with an accuracy to an order of magnitude in the range $10^{-5} \ll 1 - \chi_c \ll 1$ we have $\mathcal{T}_Q \ll 10^{-5}$ and $\Delta_f^Q, X_f^Q \ll 10^{-3}$, whereas at the critical point vicinity $1 - \chi_c \ll 10^{-5}$ we find $\mathcal{T}_Q \sim 10^{-5}$ and $X_f^Q \sim 10^{-3}$.

In quasi-2D systems at $1 - \chi_c \ll 1$ we have $\mathcal{T}_Q \sim 10^{-7}$, $\rho_f^Q \sim 10^{-4}$ where in the domain $1 - \chi_c \ll 10^{-7}$ of the self-similar ‘‘superelliptical’’ collapse the aspect ratio by the moment of front delocalization is $\mathcal{A}_Q \sim 10^{-2}$, whereas in the domain $10^{-4} \ll 1 - \chi_c \ll 1$ of the self-similar ‘‘elliptical’’ collapse the aspect ratio is $\mathcal{A}_Q \sim \sqrt{1 - \chi_c} \gg 10^{-2}$. In 3D systems, respectively, at $1 - \chi_c \ll 1$ we find $\mathcal{T}_Q \sim 10^{-6}$, $\rho_f^Q \sim 10^{-3}$ where in the domain $1 - \chi_c \ll 10^{-6}$ of the self-similar ‘‘superellipsoidal’’ collapse the aspect ratio is $\mathcal{A}_Q \sim 10^{-3/2}$, whereas in the domain $10^{-3} \ll 1 - \chi_c \ll 1$ of the self-similar ‘‘ellipsoidal’’ collapse the aspect ratio is $\mathcal{A}_Q \gg 10^{-3/2}$. Thus, we conclude that although in the quasi-1D case in the vicinity of the critical point the quantity \mathcal{T}_Q passes through a relatively sharp local maximum, at all d the front remains sharp up to a narrow vicinity of the collapse point.

B. Coalescence

1. Coalescence far away from the threshold $\Lambda \gg \Lambda_*$

Far away from the coalescence threshold $\Lambda \gg 1(T_{cl} \sim 1/\ln \Lambda \ll 1)$ according to Eqs. (74) we find that in the range $\mathcal{K} \sim 10^{16}-10^{12}$ ($d = 1, 2, 3$) at $1 \ll \sqrt{\Lambda} \ln \Lambda \ll 10^8-10^6$ the characteristic time of front delocalization is $\mathcal{T}_X^Q \sim (10^{-8}-10^{-6})\sqrt{\Lambda}$ and the characteristic length of front delocalization $X_f^Q \sim (10^{-4}-10^{-3})(\Lambda/\ln^2 \Lambda)^{1/4}$. As mentioned, in a qualitative contrast to the quasi-1D case, where the internal sea area disappears after the delocalization of the front X_f^- , in quasi-2D and 3D systems the coalescence is completed by formation of a dumbbell-like island limited by the localized front with a minimal isthmus radius ρ_f^Q in the system center $X_f = 0$. According to Eqs. (79) and (80), the characteristic time of front localization \mathcal{T}_ρ^Q and the isthmus radius ρ_f^Q are determined by the expressions

$$\rho_f^Q \sim \sqrt{\mathcal{T}_\rho^Q} \sim (10^{-4}-10^{-3})(\Lambda/\ln \Lambda)^{1/4}.$$

Since in the limit of too large $\Lambda \rightarrow \infty$ ($T_{cl}/T_c \rightarrow 0$) the majority of particles die during evolution of the formed spherical

island, we conclude that in a wide range of $\Lambda \gg 1$ the front remains sharp up to a narrow vicinity of the coalescence point.

2. Coalescence in the vicinity of the threshold $\Lambda \sim \Lambda_*$

In the quasi-1D case, in the vicinity of the coalescence threshold $10^{-5} \ll \chi_M - 1 \ll 1$ we find

$$\mathcal{T}_X^Q \ll 10^{-5}, \quad X_f^Q \ll 10^{-3},$$

whereas in the domain $\chi_M - 1 \ll 10^{-5}$ we obtain $\mathcal{T}_X^Q \sim 10^{-5}$, $X_f^Q \sim 10^{-3}$. In quasi-2D and 3D systems at $T < T_{cl}$ in the range $10^{-4}-10^{-3}$ ($d = 2, 3$) $\ll \chi_M - 1 \ll 1$ we find

$$\mathcal{T}_X^Q \ll X_f^Q \sim 10^{-4}-10^{-3},$$

whereas in the domain $\chi_M - 1 \ll 10^{-4}-10^{-3}$ we obtain $\mathcal{T}_X^Q \sim X_f^Q \sim 10^{-4}-10^{-3}$. Correspondingly, at the final stage of coalescence at $10^{-4}-10^{-3} \ll \chi_M - 1 \ll 1$ we have

$$\mathcal{T}_\rho^Q \ll \rho_f^Q \sim 10^{-4}-10^{-3},$$

whereas in a narrow vicinity of the threshold $\chi_M - 1 \ll 10^{-4}-10^{-3}$, instead of formation of an isthmus, the elastic reflection of the ‘‘relocalized’’ front is realized at the fragmentation stage $\mathcal{T}_X^Q(\text{fr}) \sim \mathcal{T}_X^Q(\text{cl})$.

C. Fragmentation

Due to narrowness of the fragmentation range, in the entire fragmentation domain $\kappa \sim \mathcal{K}$, that is why, according to Eqs. (83) and (87), not too close to the threshold points $\mathcal{T}_\rho^Q \sim \mathcal{T}_X^Q \sim 10^{-7}-10^{-6}$ and $\rho_f^Q \sim X_f^Q \sim 10^{-4}-10^{-3}$. Correspondingly, in a narrow vicinity of the coalescence threshold $1 - \chi_M \ll 10^{-4}-10^{-3}$, elastic reflection of the front occurs without coalescence, whereas in a narrow vicinity of the threshold of centers merging $\chi_s - 1 \ll 10^{-4}-10^{-3}$ (the limit of the quasi-1D string) the fragmentation is completed by disruption of the islands.

Summarizing, we conclude that during diffusion-controlled evolution of the islands, the reaction front remains sharp up to a narrow vicinity of the coalescence, fragmentation, and collapse points and, consequently, the whole picture of island evolution is self-consistent in a wide range of parameters. According to Eq. (88), with an increase in the initial particle number in the island and a corresponding increase in the initial distance between the islands, this statement only gets stronger. Moreover, due to a weak power dependence of \mathcal{T}_Q on \mathcal{K} , this statement remains valid at a significant decrease in the reaction constant.

VIII. CONCLUSION

In this paper, we have presented a systematic analytical study of diffusion-controlled evolution, coalescence, fragmentation, and collapse of two identical spatially separated d -dimensional A -particle islands in the B -particle sea at propagation of the sharp reaction front $A + B \rightarrow 0$. The obtained self-consistent picture of evolution of the islands and front trajectories is based on three central assumptions: (i) on the condition of local conservation of the difference concentration $s(\mathbf{r}, t)$ which follows from the ‘‘standard’’ requirement of equality of unlike particles diffusivities; (ii) on the assumption

that the relative front width can be neglected during islands' evolution which follows from the remarkable property of effective dynamical "repulsion" of unlike species; and (iii) on the quasistatic approximation (QSA) which allowed obtaining a self-consistent picture of front width evolution and revealing a domain of its applicability parameters. The main results can be formulated as follows:

(1) It has been established that if the initial distance between the centers of the islands 2ℓ and the initial ratio of island to sea concentrations $c = a_0/b_0$ are relatively large, the evolution of the island-sea-island system is determined unambiguously by the dimensionless parameter

$$\Lambda = \mathcal{N}_0/\mathcal{N}_\Omega,$$

where \mathcal{N}_0 is the initial particle number in the island and \mathcal{N}_Ω is the initial number of sea particles in the volume $\Omega = (2\ell)^d$.

(2) It has been shown that there is a threshold value

$$\Lambda_*(d) = (\pi e/2d)^{d/2}/2,$$

below which the islands die individually and above which island coalescence occurs.

(3) It has been established that regardless of d the centers of each of the islands move toward each other along the universal trajectory, merging in a united center at the critical value

$$\Lambda_s(d) = (\sqrt{e}/2)(\pi/2)^{d/2}.$$

In 1D systems $\Lambda_s = \Lambda_*$, that is why at $\Lambda < \Lambda_s$ each of the islands dies individually, whereas at $\Lambda > \Lambda_s$ coalescence is completed by the collapse of the single-centered island in the system center. In 2D and 3D systems in the range $\Lambda_* < \Lambda < \Lambda_s$ the coalescence is accompanied by the subsequent fragmentation (division) of the two-centered island and is completed by the individual collapse of each of the islands.

(4) It has been demonstrated that in the limit of small $\Lambda^{2/d} \ll 1$ the evolution of each of the island partners occurs autonomously in the shape of a d -dimensional sphere with the unshifted center. In the limit of large $\Lambda^{2/d} \gg 1$ the evolution of the island formed by coalescence occurs in the shape of a d -dimensional sphere with the center in the system center. In both of the limits the expansion-contraction-collapse of the island is described by the *universal* scaling law.

(5) It has been established that at any d and Λ the evolution of the island in the vicinity of the collapse point acquires a *self-similar* character. It has been shown that in 1D systems at $\Lambda \neq \Lambda_s$ "radii" of the islands Δ_\pm contract "synchronously" to the collapse point $X_c(\Lambda)$, whereas at the very critical point $\Lambda_s = \Lambda_*$ both of the islands die simultaneously with the "internal" sea area. In 2D and 3D systems at $\Lambda \neq \Lambda_s$, the island collapse occurs in the shape of an ellipse (ellipsoid of revolution) with the constant aspect ratio $\mathcal{A}(\Lambda)$ which contracts unlimitedly as Λ approaches the critical point Λ_s both from above and below (the limit of the "quasi-1D string"). At the very critical point of centers merging Λ_s the island collapse occurs in the shape of a superellipse (superellipsoid of revolution) with the aspect ratio $\mathcal{A}(\mathcal{T})$ which contracts unlimitedly with time while approaching the collapse point T_c .

(6) The laws of islands' evolution in the vicinity of the starting points of coalescence $T_{cl}(\Lambda)$ and fragmentation

$T_{fr}(\Lambda)$ have been revealed. It has been demonstrated that in 2D and 3D systems the front takes the shape of a hyperbola (hyperboloid of revolution) in the vicinity of the system center. At $T < T_{cl}$ the vertices of the hyperbola (hyperboloid) move toward each other forming at $T > T_{cl}$ a two-centered island with an increasing isthmus radius in the system center. In the vicinity of the fragmentation point, this process occurs in a reverse order. It has been shown that at the threshold point Λ_* the elastic reflection of the front occurs in the system center with an abrupt reversal of its velocity sign, and a compact description of the island fragmentation-collapse in the limit of the "quasi-1D string" $\Lambda \rightarrow \Lambda_s$ has been found.

(7) Within the QSA, the self-consistent power laws of evolution of the relative front width in the vicinity of coalescence, fragmentation, and collapse points have been revealed for quasi-1D, quasi-2D, and 3D systems. The characteristic times of front delocalization and relocalization have been obtained depending on the defining parameters of the problem. It has been shown that in the diffusion-controlled annihilation regime, the front remains sharp up to a narrow vicinity of coalescence, fragmentation, and collapse points and, consequently, the whole picture is *self-consistent* in a wide range of parameters.

As we have mentioned, because of mirror symmetry, this model simultaneously describes the evolution of the d -dimensional A -particle island in a semi-infinite B -particle sea with a reflecting $(d-1)$ -dimensional "wall". It should be emphasized, however, that as well as in Ref. [37], here the evolution of islands has been considered at equal species diffusivities. Although we believe that the regularities discovered reflect the key features of islands' evolution, the study of the much more complicated problem for unequal species diffusivities remains a challenging problem for the future. Moreover, we hope that the future extensive numerical calculations together with the corresponding experimental data will enable revealing a comprehensive picture of evolution of the front during its delocalization and allow us to reveal the limits of applicability of the macroscopic diffusion description in the vicinity of the collapse point.

In conclusion, we note that the mechanisms and regularities of coalescence and collapse of two identical spatially separated objects (liquid drops, biological cells, two-dimensional islands, black holes, neutron stars, etc.) in a foreign medium draw increased interdisciplinary interest in a wide range of applications from astrophysics, biophysics, and hydrodynamics to condensed matter physics, chemical physics, and materials science [41–50]. Depending on the nature of objects and mechanisms of direct or indirect interaction with the medium, the scenarios of coalescence and collapse, in spite of some common features, demonstrate a rich diversity. We hope that the results obtained in this work represent one of the most detailed scenarios of the coalescence, fragmentation, and collapse development, the basic features of which may turn out to be universal in a wide spectrum of reaction-diffusion systems.

ACKNOWLEDGMENT

The research is carried out within the state task of the Institute of Solid State Physics, Russian Academy of Sciences.

- [1] P. L. Krapivsky, E. Ben-Naim, and S. Redner, *A Kinetic View of Statistical Physics* (Cambridge University Press, Cambridge, 2010).
- [2] U. C. Tauber, M. Howard, and B. P. Vollmayr-Lee, *J. Phys. A: Math. Gen.* **38**, R79 (2005).
- [3] D. ben Avraham and S. Havlin, *Diffusion and Reactions in Fractals and Disordered Systems* (Cambridge University Press, Cambridge, 2000).
- [4] D. C. Mattis and M. L. Glasser, *Rev. Mod. Phys.* **70**, 979 (1998).
- [5] B. Chopard and M. Droz, *Cellular Automata Modeling of Physical Systems* (Cambridge University Press, Cambridge, 1998).
- [6] E. Kotomin and V. Kuzovkov, *Modern Aspects of Diffusion Controlled Reactions: Cooperative Phenomena in Bimolecular Processes* (Elsevier, Amsterdam, 1996).
- [7] L. V. Butov, A. C. Gossard, and D. S. Chemla, *Nature (London)* **418**, 751 (2002).
- [8] D. Snoke, S. Denev, Y. Liu, L. Pfeiffer, and K. West, *Nature (London)* **418**, 754 (2002).
- [9] S. Yang, L. V. Butov, L. S. Levitov, B. D. Simons, and A. C. Gossard, *Phys. Rev. B* **81**, 115320 (2010).
- [10] T. Antal, M. Droz, J. Magnin, and Z. Racz, *Phys. Rev. Lett.* **83**, 2880 (1999).
- [11] Z. Racz, *Physica A (Amsterdam)* **274**, 50 (1999).
- [12] S. Thomas, I. Lagzi, F. Molnar, Jr., and Z. Racz, *Phys. Rev. Lett.* **110**, 078303 (2013).
- [13] F. Brau, G. Schusztter, and A. De Wit, *Phys. Rev. Lett.* **118**, 134101 (2017).
- [14] V. Loodts, P. M. J. Trevelyan, L. Rongy, and A. De Wit, *Phys. Rev. E* **94**, 043115 (2016).
- [15] I. Mastromatteo, B. Toth, and J. P. Bouchaud, *Phys. Rev. Lett.* **113**, 268701 (2014).
- [16] L. Galfi and Z. Racz, *Phys. Rev. A* **38**, 3151 (1988).
- [17] S. Cornell and M. Droz, *Phys. Rev. Lett.* **70**, 3824 (1993).
- [18] B. P. Lee and J. Cardy, *Phys. Rev. E* **50**, R3287 (1994).
- [19] S. J. Cornell, *Phys. Rev. Lett.* **75**, 2250 (1995).
- [20] P. L. Krapivsky, *Phys. Rev. E* **51**, 4774 (1995).
- [21] G. T. Barkema, M. J. Howard, and J. L. Cardy, *Phys. Rev. E* **53**, R2017 (1996).
- [22] E. Ben-Naim and S. Redner, *J. Phys. A: Math. Gen.* **25**, L575 (1992).
- [23] Z. Koza, *J. Stat. Phys.* **85**, 179 (1996).
- [24] S. B. Yuste, L. Acedo, and K. Lindenberg, *Phys. Rev. E* **69**, 036126 (2004).
- [25] D. Froemberg and I. M. Sokolov, *Phys. Rev. Lett.* **100**, 108304 (2008).
- [26] Z. Koza and H. Taitelbaum, *Phys. Rev. E* **56**, 6387 (1997).
- [27] I. Hecht, Y. Moran, and H. Taitelbaum, *Phys. Rev. E* **73**, 051109 (2006).
- [28] I. Bena, M. Droz, K. Martens, and Z. Racz, *J. Phys.: Condens. Matter* **19**, 065103 (2007).
- [29] B. M. Shipilevsky, *Phys. Rev. E* **67**, 060101(R) (2003).
- [30] B. M. Shipilevsky, *Phys. Rev. E* **70**, 032102 (2004).
- [31] B. M. Shipilevsky, *Phys. Rev. E* **77**, 030101(R) (2008).
- [32] S. Kisilevich, M. Sinder, J. Pelleg, and V. Sokolovsky, *Phys. Rev. E* **77**, 046103 (2008).
- [33] B. M. Shipilevsky, *Phys. Rev. E* **79**, 061114 (2009).
- [34] B. M. Shipilevsky, *Phys. Rev. E* **82**, 011119 (2010).
- [35] C. P. Haynes, R. Voituriez, and O. Benichou, *J. Phys. A: Math. Gen.* **45**, 415001 (2012).
- [36] B. M. Shipilevsky, *Phys. Rev. E* **88**, 012133 (2013).
- [37] B. M. Shipilevsky, *Phys. Rev. E* **95**, 062137 (2017).
- [38] M. Fiałkowski, A. Bitner, and B. A. Grzybowski, *Phys. Rev. Lett.* **94**, 018303 (2005).
- [39] I. Lagzi, P. Papai, and Z. Racz, *Chem. Phys. Lett.* **433**, 286 (2007).
- [40] N. Withers, *Nat. Chem.* **2**, 160 (2010).
- [41] A. Abi Mansour and M. Al-Ghoul, *Phys. Rev. E* **89**, 033303 (2014).
- [42] L. V. Butov, L. S. Levitov, A. V. Mintsev, B. D. Simons, A. C. Gossard, and D. S. Chemla, *Phys. Rev. Lett.* **92**, 117404 (2004).
- [43] M. Garzon, L. J. Gray, and J. A. Sethian, *Phys. Rev. E* **97**, 033112 (2018).
- [44] T. Dessup, C. Coste, and M. Saint Jean, *Phys. Rev. E* **95**, 012206 (2017).
- [45] J. Zhang, L. Chen, and M.-J. Ni, *Phys. Rev. Fluids* **4**, 043604 (2019).
- [46] N. S. Shuravin, P. V. Dolganov, and V. K. Dolganov, *Phys. Rev. E* **99**, 062702 (2019).
- [47] S. Perumanath, M. K. Borg, M. V. Chubynsky, J. E. Sprittles, and J. M. Reese, *Phys. Rev. Lett.* **122**, 104501 (2019).
- [48] C. M. Caragine, S. C. Haley, and A. Zidovska, *Phys. Rev. Lett.* **121**, 148101 (2018).
- [49] A. Gupta, B. Krishnan, A. B. Nielsen, and E. Schnetter, *Phys. Rev. D* **97**, 084028 (2018).
- [50] C. Reisswig, C. D. Ott, E. Abdikamalov, R. Haas, P. Mosta, and E. Schnetter, *Phys. Rev. Lett.* **111**, 151101 (2013).